

**PREPARATION OF CO₂-SWITCHABLE POLY(METHYL
METHACRYLATE) LATEXES BY SURFACTANT-FREE
EMULSION POLYMERIZATION**

by

Haixia Jin

A thesis submitted to the Department of Chemical Engineering

In conformity with the requirements for

the degree of Master of Applied Science

Queen's University

Kingston, Ontario, Canada

(September, 2014)

Copyright ©Haixia Jin, 2014

Abstract

The work presented herein focused on the preparation of CO₂ switchable poly(methyl methacrylate) latexes by surfactant-free emulsion polymerization. N,N-Dimethylaminoethyl Methacrylate (DMAEMA) was chosen as the functional comonomer to act as an in-situ generated surface active agent as well as the CO₂ responsive agent. The azo initiator 2,2'-azobis[2-(2-imidazolin-2-yl)propane]dihydrochloride (VA-044) also partially contributed to both the stabilization and the CO₂ switchability. DMAEMA was first protonated by HCl during the emulsion polymerization to prevent hydrolysis and enhance DMAEMA partitioning into the water phase. Two switching on/off cycles were conducted to the latex obtained from the surfactant-free emulsion polymerization. The first switching-off cycle was carried out by NaOH neutralization, followed by simple CO₂ purging for redispersion. Full recovery of particle size and distribution, solids content and latex stability was achieved within 5 min of applying the triggers. The second switching cycle was carried out by alternating N₂/CO₂ purging. Sonication was not needed in each switching-on process (a significant and important improvement over previous work in the Cunningham and Jessop groups). A ratio of VA-044:DMAEMA within the range of 1:8~1:2, a minimum overall N% ($N_{\text{DMAEMA}}+N_{\text{VA-044}}$) at 1% and a maximum solids content at 20% were the required conditions in order to make latex successfully recover from two switching cycles. Systematic particle size manipulation was carried out by varying temperature, VA-044:DMAEMA ratio and solids content. A wide size range 170~500 nm was achieved, allowing for multiple potential applications.

Co-Authorship

The bulk of research was completed independently by myself, under the supervision of Dr. Michael Cunningham. The preparation and editing of this thesis was conducted under the supervision of Dr. Michael Cunningham.

Acknowledgements

A sincere Thank-You to Dr. Michael Cunningham for his guidance and encouragement during the past two years: It was my honor and pleasure to learn from Mike and graduate with a fraction of his knowledge and always positive attitude. I also greatly appreciate his generous offerings to participate in high level international conferences and workshops during my Master's and the extensive opportunities and friendships established during these conferences. I want to thank Dr. Philip Jessop for his continuous advice and input into my project and the Queen's Polymer Group behind the cooperation between the Cunningham Group and Jessop Group.

I want to express my gratitude to my family back in China for their understanding and respect of my life and career choices. Being the only daughter away from her family, I want to thank my parents for letting me stand on my own feet and for the fine family education that enables me to be curious and independent.

It is my pleasure to meet all the great friends and coworkers in Kingston and share two years of a tasty journey. Thanks to members in the Cunningham Group Abbas, Ali (D), Sean, Oxana, Omar, Roberto, Su, Haidong, Aaron, Vitaliy, Eli, Kyle, Ryan, Jennifer, and Hutchison Group Kevin, Ali (P), Calista, Thomas, Weiwei, Jan and everyone in CHEE Yutian, Eric (Peterson), Eric (Potter), Antonio, Praf, Lydia, Ming, Jasmine, Stu (B), Stu (Y)... for your kind help and wonderful conversations on either science or culture, music, politics, history, food and gardening. I look forward to seeing everyone in our professional network in the near future.

Thanks to Dawn for organizing my grand travels, Kalam for training on various instruments and Pascal for his short period of experimental assistance on NMR work. Steve and Kelly, thanks for the constant effort to ensure a safe and pleasant working environment.

Thanks to Dr. Francoise Sauriol for being the living library of NMR techniques. Its versatility still amazes me every now and then even after 5 years using it. Thanks to Dr. Yan for the help with SEM and TEM.

Special thanks to Oxana and Mastouerh for your precious presence in my early twenties with all the life lessons and wisdom.

(Thanks to Timber, Chopin and Mozart for the pleasant company.)

I would like to recognize the Ontario Green Chemistry and Green Engineering Research Chair (Cunningham) and Natural Sciences and Engineering Research Council of Canada (NSERC) for financial support.

Special thanks to the International Polymer Colloids Group (IPCG) for the wonderful science and the tremendous community fun. The short period of mentorship from the great emulsion scientists Dr. Dieter Urban, Dr. Bernd Reck, Dr. Peter Lovell, Dr. Mohamed El-Aasser, Dr. Stefan Bon, Dr. Michael Monteiro, Dr. Mitchell Winnik, Dr. Alex Van Herk...has brought in so many precious perspectives in my research and career.

“Among all the difficulties lies the opportunity.”

Table of Content

| | |
|--|------|
| Abstract..... | ii |
| Co-Authorship | iii |
| Acknowledgements..... | iv |
| List of Figures..... | ix |
| List of Tables | xi |
| List of Schemes..... | xii |
| List of Abbreviations | xiii |
| Nomenclature..... | xiv |
| Chapter 1 Introduction..... | 1 |
| 1.1 Overview..... | 1 |
| 1.2 Research objectives..... | 2 |
| Chapter 2 Literature Review..... | 3 |
| 2.1 Free radical polymerization | 3 |
| 2.1.1 Copolymerization..... | 3 |
| 2.2 Emulsion polymerization | 4 |
| 2.2.1 Mechanisms, kinetics and general features of emulsion polymerization..... | 4 |
| 2.2.2 Latex stability and zeta-potential | 7 |
| 2.2.3 Particle size, particle size distribution and number of particles..... | 8 |
| 2.3 Surfactant-free emulsion polymerization..... | 10 |
| 2.3.1 Nucleation mechanism in SFEP..... | 10 |
| 2.3.2 General features of SFEP..... | 12 |
| 2.3.3 Functional comonomers in SFEP..... | 13 |
| 2.4 CO ₂ -switchable polymers | 13 |
| 2.4.1 CO ₂ -switchable surface active agent..... | 14 |
| References..... | 18 |
| Chapter 3 CO ₂ -Switchable PMMA Latexes with Controllable Particle Size Prepared by Surfactant-Free Emulsion Polymerization..... | 22 |
| Abstract..... | 22 |
| 3.1 Introduction..... | 23 |
| 3.2 Experimental Methods | 24 |
| 3.2.1 Materials | 24 |
| 3.2.2 Surfactant-free emulsion polymerization using VA-044 and DMAEMA | 24 |

| | |
|---|----|
| 3.2.3 Coagulation and redispersion of latex..... | 25 |
| 3.2.4 Characterization | 25 |
| 3.3 Results and discussions..... | 27 |
| 3.3.1 Surfactant-free emulsion polymerization of methyl methacrylate..... | 27 |
| 3.3.1.1 Effect of VA-044:DMAEMA ratio on latex properties | 28 |
| 3.3.1.2 Effects of varying the overall amount of stabilizing force..... | 34 |
| 3.3.1.3 Effects of varying solids content (initial monomer concentration)..... | 38 |
| 3.3.1.4 Effects of varying reaction temperatures at different solids content..... | 39 |
| 3.3.1.5 Summary of controlling the particle size range | 42 |
| 3.3.2 CO ₂ -switchable performance of PMMA latexes prepared from SFEP | 43 |
| 3.3.2.1 Boundary conditions for achieving CO ₂ -switchable behavior..... | 48 |
| 3.4 Conclusion | 49 |
| References..... | 51 |
| Chapter 4 A comprehensive characteristic study of functional comonomer DEAEMA/DMAEMA used in surfactant-free emulsion polymerization | 53 |
| Abstract..... | 53 |
| 4.1 Introduction..... | 54 |
| 4.2 Experimental Section | 54 |
| 4.2.1 Materials | 54 |
| 4.2.2 Determination of protonation efficiency and hydrolysis degree by ¹ H NMR..... | 54 |
| 4.2.3 Surfactant-free emulsion polymerization using VA-061/VA-044 and DEAEMA | 55 |
| 4.3 Characterization | 56 |
| 4.4 Results and discussion | 57 |
| 4.4.1 Surfactant-free emulsion polymerization using VA-044/VA061 and DEAEMA..... | 57 |
| 4.4.2 Determination of protonation efficiency of DMAEMA by ¹ HNMR | 61 |
| 4.4.3 Determination of monomer hydrolysis of DEMA/DMAEMA by ¹ HNMR | 65 |
| 4.5 Conclusion | 70 |
| References..... | 72 |
| Chapter 5 Conclusions and recommendations for future work..... | 73 |
| 5.1 Conclusions..... | 73 |
| 5.2 Recommendations for future work | 74 |
| 5.2.1 Continuing the use of azo initiators | 74 |
| 5.2.2 Developing more techniques for surface group characterization..... | 74 |
| 5.2.3 Introducing new functional monomers as CO ₂ responsive agent | 75 |

| | |
|--|----|
| 5.2.4 Extension to more emulsion techniques..... | 76 |
| 5.2.5 Exploring low T_g materials | 76 |
| 5.2.6 Potential application in drug delivery systems for cancer therapy..... | 76 |
| 5.2.7 High pressure CO_2 atmosphere for DMAEMA/DEAEMA systems | 77 |
| Appendix A..... | 78 |
| Appendix B | 80 |
| Appendix C..... | 82 |

List of Figures

| | |
|--|----|
| Figure 2.1 Three stages of emulsion polymerization and their schemed kinetics ⁶ | 6 |
| Figure 2.2 Mechanism of particle formation for SFEP of St/4-VP/APS system | 12 |
| Figure 2.3 Latex stabilized by CO ₂ -switchable surfactant on(A)/off(B) forms ⁵⁷ | 15 |
| Figure 3.1 Particle size versus VA-044mol% / DMAEMAmol% with fixed total N ⁺ at 2mol% ... | 31 |
| Figure 3.2 Number of particles and total stabilized surface area with increasing percentage of VA-044 at fixed number of total N ⁺ (2mol%)..... | 32 |
| Figure 3.3 Monomer conversion versus time at the early stages of polymerization at 55 °C with initiator concentrations at 0.1mol% (F-1), 0.4mol% (F-2), 0.7mol% (F-3) and 1.0mol% (F-4) ... | 33 |
| Figure 3.4 Particle size versus total N ⁺ % at constant V:D ratio 1:3 (Series O) | 36 |
| Figure 3.5 Particle size versus concentration of DMAEMA at constant VA-044 level (Series I). 36 | |
| Figure 3.6 Particle size versus concentration of VA-044% at constant DMAEMA levels (0.6%, 1.8% and 2.4%, respectively) | 37 |
| Figure 3.7 Theoretical modeling of temperature dependence of VA-044 decomposition..... | 40 |
| Figure 3.8 Monomer conversion of Entry S-2/N-2 vs. reaction time | 40 |
| Figure 3.9 Particle size (left) and PDI (right) variation with solids content at 65 °C and 75 °C | 42 |
| Figure 3.10 Summary of upper/lower range of particle size by varying parameters (nm) | 43 |
| Figure 3.11 DLS results and photographs of two switching-off/on cycles of Entry N-5 | 47 |
| Figure 4.1 Bimodal size distribution of B-1 (531 nm/55.4%; 3857 nm/44.6%)..... | 61 |
| Figure 4.2 Standard curve of HCl protonation of DMAEMA | 62 |
| Figure 4.3 Calculation of protonation efficiency of DMAEMA at CO ₂ saturated acidity at room temperature (94%) | 63 |
| Figure 4.4 DMAEMA hydrolysis at 65 °C in CO ₂ saturated aqueous phase within 4h (pH=7.14) 67 | |
| Figure 4.5 Temperature dependence of hydrolysis of DEAEMA/DMAEMA at CO ₂ saturated acidity (M:DMAEMA; E:DEAEMA) | 67 |
| Figure 4.6 Hydrolysis of 84% HCl protonated DMAEMA (12%, pH=7.41) | 68 |
| Figure 4.7 Hydrolysis degree under CO ₂ /HCl protonation at pH/temperature conditions | 69 |
| Figure 5.1 Two switching cycles of CO ₂ -switchable PMMA latex (Entry N-5) | 73 |
| Figure 5.2 NMR determination of hydrolysis degree of N-[3-(dimethylamino) propyl] methacrylamide..... | 75 |
| Figure B.1 ln[DMAEMA/DEAEMA] vs. time at room temperature | 80 |
| Figure B.2 ln[DMAEMA/DEAEMA] vs. time at 45 °C | 81 |

Figure B.3 $\ln[\text{DMAEMA}/\text{DEAEMA}]$ vs. time at 65°C 81

List of Tables

| | |
|--|----|
| Table 2.1 Typical particle size ranges in different emulsion techniques ¹⁶ | 9 |
| Table 2.2 Summary of different types of responsive surfactants | 14 |
| Table 3.1 SFEP recipe and latex properties with constant concentration of overall functional groups at 65 °C | 29 |
| Table 3.2 GPC results of N-Series on molecular weight, PDI and initiation efficiency | 30 |
| Table 3.3 SFEP recipe and latex properties with calibrated ionic strength at 65 °C | 34 |
| Table 3.4 SFEP recipe and latex properties with fixed V:D ratio (1:3) with varied overall N ⁺ % . | 35 |
| Table 3.5 SFEP recipe and latex properties with varied amount of DMAEMA at 65 °C | 35 |
| Table 3.6 SFEP recipe and latex properties with different solid content at 65 °C | 38 |
| Table 3.7 SFEP recipe and latex properties with different solids content at 75 °C(S)/65°C(M) ... | 41 |
| Table 3.8 Latex properties of CO ₂ -switchable cycles (N-Series) | 46 |
| Table 3.9 Latex properties during switching cycles (O-3 & S-4) | 49 |
| Table 4.1 The seeds properties under different DEAEMA:VA-061 ratio | 58 |
| Table 4.2 Comparison of latex properties under CO ₂ and HCl protonation | 59 |
| Table 4.3 Temperature dependence of protonation of DMAEMA at CO ₂ saturated acidity | 64 |
| Table 4.4 Rate constants and half-life of hydrolysis of DMAEMA/DEAEMA | 68 |
| Table A.1 Zeta-potential measurement using dip cell/ disposable zeta cell | 78 |
| Table A.2 Effect of sample concentration on particle size | 78 |
| Table C.1 Particle size results of replicate runs | 82 |

List of Schemes

| | |
|--|----|
| Scheme 2.1 Reversible transformation between amidine and its amidinium bicarbonate ⁵⁷ | 15 |
| Scheme 2.2 Protonation/deprotonation of switchable initiator VA-061 and DEAEMA | 17 |
| Scheme 3.1 Structures of VA-044 (left) and protonated | 28 |
| Scheme 3.2 Switching-Off/On cycles in molecular perspective..... | 45 |
| Scheme 4.1 NMR peak assignment in DMAEMA | 63 |
| Scheme 4.2 Hydrolysis of DMAEMA/DEAEMA (DEAEMA shown by dashed line)..... | 65 |
| Scheme 4.3 NMR peak assignment for DMAEMA hydrolysis | 66 |
| Scheme 4.4 Ring Formation of DMAEMA upon HCl and CO ₂ Protonation..... | 68 |

List of Abbreviations

| | |
|--------|--|
| 4-VP | 4-Vinylpyridine |
| APS | Ammonium persulphate |
| CMC | Critical micelle concentration |
| DEAEMA | N,N-diethylaminoethyl methacrylate |
| DLS | Dynamic light scattering |
| DMAEMA | N,N-dimethylaminoethyl methacrylate |
| EDL | Electronic double layer |
| GPC | Gel permeation chromatography |
| KPS | Potassium persulfate |
| LCST | Lower critical solution temperature |
| MMA | Methyl methacrylate |
| NMR | Nuclear magnetic resonance |
| PDI | Polydispersity index |
| PMMA | Poly(methyl methacrylate) |
| PS | Polystyrene |
| PSD | Particle size distribution |
| PVAc | Poly(vinyl acetate) |
| SFEP | Surfactant-free emulsion polymerization |
| St | Styrene |
| SLS | Sodium lauryl sulfate |
| THF | Tetrahydrofuran |
| VA-044 | 2,2'-azobis[2-(2-imidazolin-2-yl)propane]dihydrochloride |
| VA-061 | 2,2'-azobis[2-(2-imidazolin-2-yl)propane] |

Nomenclature

| | |
|--------------|--|
| k_p | Propagation rate coefficient [$L \cdot mol^{-1} \cdot s^{-1}$] |
| $[M]_p$ | Monomer concentration [$mol \cdot L^{-1}$] |
| d_z | Diameter of the particle [nm] (intensity value from DLS) |
| f | Initiation efficiency |
| k_h | Rate of hydrolysis [s^{-1}] |
| $M_{n/GPC}$ | Number average molecular weight from GPC [$g \cdot mol^{-1}$] |
| n | Number of radicals per polymer particle |
| N_A | Avogadro constant |
| | Mole percent of tertiary amine groups in DMAEMA with respect to MMA |
| N_{DMAEMA} | (=DMAEMAmol%) |
| N_p | Number of particles |
| N_{VA-044} | Mole percent of amidine groups in VA-044 with respect to MMA (=2×VA-044mol%) |
| pK_a | Acid dissociation constant |
| pK_{aH} | pKa of the conjugated acid |
| r_1, r_2 | Reactivity ratio |
| R_p | Polymerization rate [$mol \cdot L^{-1} \cdot s^{-1}$] |
| T_g | Glass transition temperature [K] |
| V:D | Mole ratio of VA-044 versus DMAEMA |
| δ | Chemical shift [ppm] |
| ζ | Zeta potential [mV] |
| χ | Mole fraction of functional group |
| ρ_p | Density of the polymer [g/cm^3] |

Chapter 1

Introduction

CO₂-switchable technologies have attracted increasing interest among both academic and industrial researchers. The utilization of the chemically benign trigger CO₂ could greatly reduce the environmental footprint in many applications including oil refining, coatings, consumer goods and controlled drug release. The application of CO₂-switchable technologies to latex systems has created novel features to switch the colloidal stability by simple gas purging, which could potentially lead to cost and energy savings in long distance latex transportation, and in other applications such as moisture-repellent coatings.

1.1 Overview

In this work, surfactant-free emulsion polymerization was used for the preparation of CO₂ switchable poly(methyl methacrylate) latex. Apart from obtaining good CO₂-switchability, control over the latex properties was set to be the other major goal, including for example high monomer conversion, small particle size, narrow particle size distribution, good latex stability and reasonable solids content (10%~20%). The dependence on sonication for redispersion remained one of the major challenges towards the industrial application of CO₂ switchable latex because of its energy intensive nature. Therefore, developing latexes that could be redispersed without requiring sonication was another major objective.

A comprehensive literature review is presented as Chapter 2, which covers fundamental aspects of an emulsion system including particle size controlling methods, the parameters contributing to latex stability and the nucleation mechanism of a surfactant-free emulsion system. The development and challenges of CO₂ switchable technologies are also reviewed. A more targeted review on CO₂ switchable latexes is included in Chapter 3.

The preparation of a series of CO₂-switchable latexes and the challenge of eliminating the need for sonication in the redispersion process is addressed in Chapter 3. The latex products demonstrated fast response to both CO₂ and N₂ triggers (within 5 min), and the particle size and distribution, solids content and colloidal stability could be fully recovered. An effort to control the particle size by tuning pH, temperature, monomer ratio and solids content is also discussed. Limiting conditions such as the highest solids content achievable and lowest amount of cationic ingredients needed to maintain latex stability and CO₂ response are also explored.

Chapter 4 serves as supplementary information to Chapter 3 with careful characterization of the functional monomers used in the proposed surfactant-free emulsion polymerization. The choice of HCl protonation during the emulsion polymerization is a method to prevent the high degree of monomer hydrolysis. Chapters 3 and 4 answer the key question why emulsion systems often exhibit inferior performance under CO₂ protonation compared to HCl protonation.

A summary of the thesis research and recommendations for future work are presented in Chapter 5. Further understanding of the mechanism of the switching processes is still needed, especially the development of proper characterization methods to determine the nature of the surface groups on the particles under switching-on and switching-off conditions. This will allow more specific control over each switching cycle and introduce more opportunities for the application of CO₂ switchable technology in emulsion systems.

1.2 Research objectives

- Apply CO₂-switchable techniques in MMA surfactant-free emulsion polymerizations and prepare stable PMMA latexes with monomer conversion above 90%.
- Achieve relatively small particle size (for a surfactant-free emulsion system) in the range 100 nm~200 nm.
- Reduce response time for switching using the triggers CO₂ and N₂.
- Eliminate sonication from the redispersion process.

Chapter 2

Literature Review

2.1 Free radical polymerization

Free radical polymerization is a common industrial process for polymer manufacturing. It usually involves an initiation stage triggered by heat, light or a redox reaction, where free radicals are produced, followed by a propagation stage where monomer units sequentially add onto the free radicals at a rate on the order of milliseconds,¹ and ends with combination/disproportionation of two radicals, i.e. the termination stage. The initiation rate coefficient and propagation rate coefficient (k_p) are among the most important factors that determine the order of magnitude of the overall polymerization rate. For the main monomer employed in our system (methyl methacrylate), an experimentally based equation was used to calculate k_p at different reaction temperatures.² Chain transfer to solvent could be of interest in a solvent-based polymerization environment. The chain transfer constant of methyl methacrylate to water is reported to be negligible.³

2.1.1 Copolymerization

Blending monomers for copolymerization is often done to tune particular properties such as glass transition temperature (T_g), chemical or weathering resistance, polarity or solubility. Introducing minor amounts of a second monomer can sometimes apply new features to the final polymer product that could not be achieved by homopolymerization. The sequence of monomers in the resulting copolymer is determined by the reactivity ratio (r_1, r_2) of the monomers, following the Mayo-Lewis equation. Reactivity ratios of the monomer pairs DMAEMA ($r_1=0.88$) and MMA ($r_2=1.12$)⁴ as well as DEAEMA ($r_1=0.94$) and MMA ($r_2=0.99$)⁵ were reported. However, these ratios could be altered in different chemical environments. For example, an acidic environment

could lead to monomer protonation which could alter the copolymerization behavior, as well as monomer partitioning between organic and aqueous phases.

2.2 Emulsion polymerization

Emulsion polymerization is widely practiced in industry. Its water-based operation promotes lower viscosity for more effective agitation, superior heat transfer for ease of temperature control and subsequently improved kinetic control compared to bulk polymerization, as well as less of an environmental footprint compared to volatile organic solvents based solution polymerization. Extensive opportunities to modify the composition and morphology of the final polymers are provided by versatile techniques such as semi-batch or continuous emulsion polymerization as well as miniemulsion and microemulsion polymerization. The latex products prepared from emulsion polymerization find applications in coatings, paints, adhesives and cosmetics or they can be post-processed as waterborne polymer resins for production of polydiene-based rubbers and major plastics such as poly (vinyl acetate), poly(chloroprene), and poly (acrylic ester) copolymers.⁶

2.2.1 Mechanisms, kinetics and general features of emulsion polymerization

A conventional emulsion polymerization system consists of a relatively hydrophobic monomer, an either water-soluble (e.g. potassium persulfate, KPS) or oil soluble (e.g. 2,2'-azobisisobutyronitrile, AIBN) initiator, surfactant(s) and water. The amphiphilic surfactant can be either physically absorbed or chemically bonded onto the particle surface. It can effectively stabilize the monomer droplets (1~10 μm in diameter, $10^{12}\sim 10^{14}$ per liter in number),⁷ be dispersed in the aqueous phase, as well as in micelles (5~10 nm in diameter, $10^{19}\sim 10^{21}$ per liter in number)⁷ when the concentration is above the critical micelle concentration (CMC). The overall surface area of micelles is much larger than that of the monomer droplets. This further enables the efficient capture of the radicals in the aqueous phase by micelles. Once the micelle is entered by a radical, it serves as a micro-batch reactor and becomes a polymer particle (0.05~1 μm in diameter,

$10^{16}\sim 10^{18}$ per liter in number)⁷ as the polymerization proceeds. The monomer droplets act as reservoirs constantly feeding monomers into micelles/particles by diffusion through the continuous phase. Predominant nucleation by micelles is termed micellar nucleation^{8,9} and occurs when the concentration of surfactant is above the CMC. When the concentration of the surfactant is below the CMC or in the case of more hydrophilic monomers, homogenous nucleation¹⁰⁻¹² becomes dominant. The oligomers grow to a critical chain length at which water solubility is no longer maintained, precipitate from the aqueous phase and aggregate with other oligomers to form primary particles. These primary particles are thermodynamically unstable, and further combine with each other and absorb surfactant to form polymer particles.

The nucleation stage (Interval I) usually only takes up 10~20%⁷ of monomer conversion, and ends with the disappearance of micelles in the system, which are either converted into polymer particles or disassembled and redistributed to supply the surfactants to other surfaces. The following particle growth stage, also termed as Interval II, is where the majority of monomer is consumed, ranging from 5%~10% to 30%~70%.⁶ The commonly applied kinetics during this stage is the Smith-Ewart model,⁸ and the rate of polymerization can be calculated as follows:

$$R_p = k_p [M]_p (nN_p / N_A) \quad (2.1)$$

Where R_p , k_p , $[M]_p$, n , N_p , N_A are the polymerization rate, propagation rate constant, monomer concentration, number of radicals per polymer particle, number of particles and Avogadro constant, respectively.

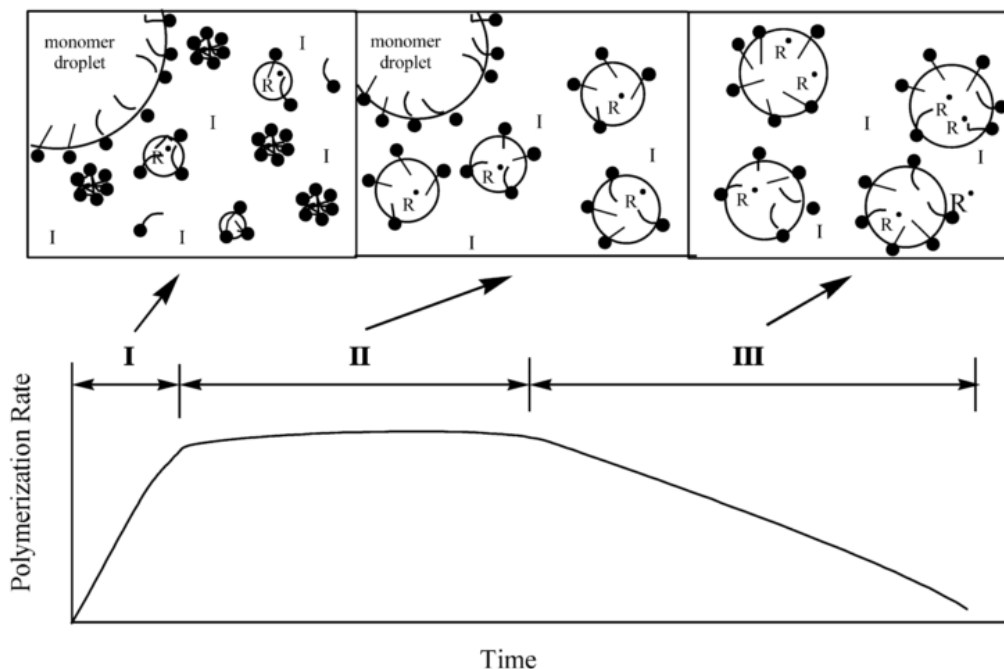


Figure 2.1 Three stages of emulsion polymerization and their schemed kinetics⁶

In bulk polymerization, increasing polymerization rate (by increasing the initiator concentration) usually means decreasing the molar mass, while in emulsion polymerization a high molecular weight and a fast polymerization rate can be simultaneously obtained. This is mainly attributed to the compartmentalization effect. According to the Smith-Ewart model case 2, the latex particles will either have one or zero radicals (average $n \sim 0.5$), under the assumption that radical termination within the particle is instantaneous and radical exit is negligible. Since the particle is also saturated by sufficient monomer supply, a steady rate of polymerization is preserved until the monomer droplets are exhausted, which signifies the end of Interval II. During Interval III the rest of the monomer inside the particles is consumed by reaction accompanied by a drop in polymerization rate due to the decreasing monomer concentration (Figure 2.1).

2.2.2 Latex stability and zeta-potential

Latex stability, usually referring to the ability of a colloidal system sustaining a state where individual particles can remain single entities, is mainly attributed to two factors:¹ 1) Brownian motion of the particles and; 2) External conditions that help stabilize the dispersion, such as high temperature, high shear and addition of stabilizers. Thermodynamically, particles in a colloidal system are always prone to coagulation ($\Delta G < 0$) in order to reduce the total particle-water interfacial area. Adding surfactant is an effective way to stabilize the system as it significantly reduces the interfacial energy. In industrial polymer manufacturing via emulsion polymerization, there is always a trade-off (in terms of the amount of added surfactant) between long-term storage stability, also known as shelf life, and the properties of the final products such as water-resistance and adhesion strength.

Synthetic strategies play a leading role in determining the latex stability by modifying the surface properties of the particles, which can be either physical absorption of additional surfactants or covalent bonding of residual initiator groups, polymeric surfactants and specific monomers onto the particle surface. There are two major stabilizing forces in opposing the van der Waals attractive force¹³ that pulls particles together: (1) electrostatic repulsion between adjacent particles provided by ionic stabilizing agents and; (2) a steric barrier that often involves hydrophilic polymer chains extending into the aqueous phase.

The classic electrical double layer (EDL) model is used to describe the electrostatic stabilization mechanism, defined as a layer of non-uniformly distributed ions surrounding the particles,¹⁴ which consists of particle surface charges, i.e. the Stern layer, and the parallel associated counter ions in the continuous aqueous phase, termed as the diffuse layer. The latter can be quantified by the well-known Debye–Hückel Equation, as follows:

$$\psi(x) = \psi_0 \exp(-\kappa x) \tag{2.2}$$

Where $\psi(x)$ is the electrical potential at a distance x from particle surface, ψ_0 is the surface potential and κ is defined as the reciprocal thickness of the diffuse electrical double layer. According to the equation, the electrical potential is determined by the distance from the particle surface and κ , both exponentially, which can be further determined by Equation (2.3):¹³

$$\kappa = \sqrt{\sum e z_i^2 n_0 / \epsilon_0 \epsilon_r k T} \quad (2.3)$$

Where $e, z_i, n_0, \epsilon_0, \epsilon_r, k, T$ are the charge of an electron, the valency and number of ion i , the dielectric constant of a vacuum and the relative dielectric constant of the medium, Boltzmann constant and temperature in Kelvin, respectively.

Therefore, with the three non-constant parameters in the equation z_i, n_0, T , the compression of the diffuse electrical double layer (a reduced $1/\kappa$), can be a consequence of using higher valency counter ions, increasing the concentration of the electrolytes or lowering the temperature, and subsequently resulting in a decrease of the colloidal stability ($\psi(x)$, Eq. 2.2). The combined effect of valency and concentration of electrolytes can also be presented as the influence of ionic strength, which, if increased, will result in a thinner layer of counter ions. Lowering the temperature slows down the thermodynamic motion internally stabilizing the particles.

Zeta-potential (ζ , mV) is defined as the potential at the Stern Plane¹⁵. ζ is positive if the potential increases from the continuous phase towards the interface. Zeta-potential is widely considered as an analytical indicator of latex stability in an electrostatically stabilized colloidal system as it is readily measurable. A colloidal system with ± 30 mV zeta-potential can be regarded as moderately stable.

2.2.3 Particle size, particle size distribution and number of particles

Among the major latex properties, particle size, size distribution and number of particles are the crucial ones that directly affect the end use of the latex products. For example, applications such

as coatings and adhesives require large surface area to promote film forming where smaller particle size and larger population of particles are desired. The general particle size obtained via conventional emulsion polymerization is usually in the range of 50~300 nm, which can be further tuned by different emulsion procedures and techniques (Table 2.1).

Table 2.1 Typical particle size ranges in different emulsion techniques¹⁶

| Emulsion Techniques | Emulsion | Miniemulsion | Microemulsion | Inverse emulsion | Surfactant-free emulsion |
|----------------------------|----------|--------------|---------------|------------------|--------------------------|
| Typical Particle Radius/nm | 50-300 | 50-500 | 10-30 | 100-1000 | 100-1000 ¹⁷ |

Nucleation controls the particle formation and is the key stage in determining the final particle size and distribution, which is heavily dependent on the polymerization mechanism. The nature and concentration of the initiator, surfactant and monomer as well as operational parameters such as temperature, agitation, ionic strength and co-solvent all affect the nucleation process. Smith and Ewart⁸ reported that the number of particles was proportional to the 0.4 power of the rate of initiation and the 0.6 power of the surfactant concentration in a styrene system at low conversion, indicating that higher surfactant levels could promote particle generation and therefore decrease the particle size, while greater availability of initiator could also contribute to smaller particle size by initiating more particles. It has been extensively reported¹⁸⁻²¹ that the increase of surfactant concentration could stabilize more surface area and thus create larger population of particles and smaller particle size. It is especially influential in the nucleation stage as it controls the availability of the overall stabilizing potential. The solubility of monomer determines the available amount of monomer in the aqueous phase.²² Particle size dependence on temperature is closely related to the rate of initiation. Particle size decreases at higher temperature, accompanied by narrower particle size distribution.²³ Gardon²⁴ reviewed experimental statistics reported in the literature on the methyl methacrylate (MMA)/sodium lauryl sulfate (SLS)/K₂S₂O₈ and the

styrene/SLS/K₂S₂O₈ systems, and presented a convenient calculation model of particle size and number of particles at any given temperature, concentration of surfactant and initiator concentration. Co-solvent addition, acetone or methanol,^{25,26} increased the solubility of the monomer while agitation enhanced mass transfer, both contributed to the particle generation. High ionic strength²⁷ reduced the thickness of the electrostatic double layer and tended to increase particle size and destabilize the latex.

2.3 Surfactant-free emulsion polymerization

In conventional emulsion polymerization, employing surfactant for stabilization is the common practice. The adsorption of surfactant onto the polymer particles may affect the properties of the resulting latex in terms of apparent diameter in suspension, surface charge, optical performance or water resistance, while attempting to remove the surfactant either by dialysis or desorption can lead to coagulation or flocculation.

Surfactant-free emulsion polymerization (SFEP), also noted as soap-free emulsion polymerization or emulsifier-free emulsion polymerization, is an emulsion technique carried out without added surfactant. In 1965, Matsumoto and Ochi²⁸ showed that monodispersed polystyrene (PS), poly(methyl methacrylate) (PMMA) and poly(vinyl acetate) (PVAc) latexes could be prepared by emulsion polymerization in the absence of added surfactant, taking advantage of the electrostatic repulsion on the particle surface resulting from the residual ionic group of potassium persulfate (KPS), the free-radical initiator. The absence of surfactant provides better moisture-resistance properties, prevents surfactant migration after film formation and preserves a clean surface with functional groups for biomedical or catalytic support applications.

2.3.1 Nucleation mechanism in SFEP

The micellar nucleation mechanism was ruled out in surfactant-free emulsion polymerization as there were no surfactants to form micelles. A “coagulative nucleation” theory that nucleation took

place by precipitation of macroradicals/macromolecules^{12,29-32} was commonly discussed. In the example of potassium persulfate initiated system, oligomers with a hydrophilic SO_4^{2-} end group were formed by homogenous propagation of the primary radicals generated by initiator decomposition in the aqueous medium and utilizing the portion of monomers dissolved in water. Once a critical chain length (60-80 units for MMA,³³ 5 units for styrene³⁴) required to maintain solubility in water was being exceeded, primary precursors precipitate from the aqueous phase and form the initial particles with very small diameter (~5 nm in the case of polystyrene),³² which are unstable and coagulate into larger entities until the electronic density on the surface became adequate to stabilize the particle. Polymer latexes prepared by amidinium-azo initiators to produce positively charged particles in surfactant-free emulsion polymerization were studied by Goodwin³⁵ et al.. Another approach is to incorporate ionic comonomer³⁶ or copolymerize non-ionic monomer pairs³⁷ to form amphiphilic copolymers. In situ formation of surface-active oligomers that are capable of self-assembling to form micelles was proposed to be the driving force of stabilizing the polymer particles. A model scheme (Figure 2.2) proposed by Yan³³ when studying the mechanism of SFEP of the styrene/4-vinylpyridine system initiated by APS suggested that oligomers formed at the early stage of SFEP were responsible for the micellization-type of nucleation. The oligomeric particles served as an emulsifier reservoir providing stabilizing agents for the monomer swollen particles as well as the monomer droplets. GPC evidence that the presence oligomers with a molecular weight ~1000 in the early stages of polymerization was used to support the micelle nucleation theory in studies on hydrophilic comonomers (vinyl acetate or methyl methacrylate) in SFEP.²⁵

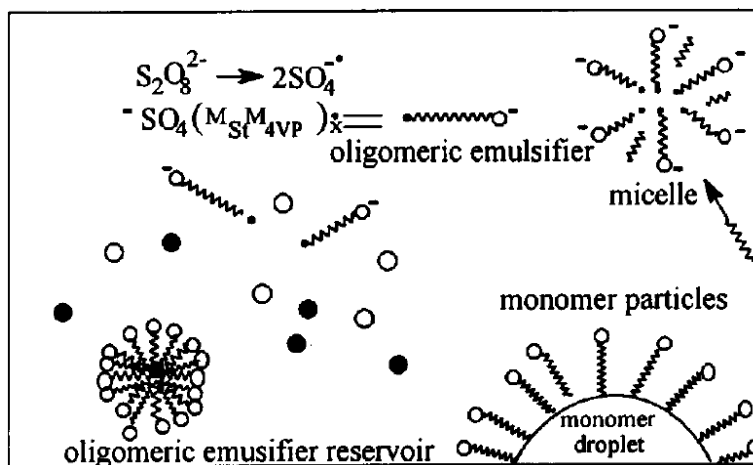


Figure 2.2 Mechanism of particle formation for SFEP of St/4-VP/APS system

2.3.2 General features of SFEP

Latexes prepared with surfactant-free emulsion polymerization exhibit several features that distinguish them from conventional emulsion polymerization. One characteristic is that the number of particles per unit water is generally lowered by up to 2 orders of magnitude compared to the typical emulsion polymerization process.³⁸ This usually leads to larger particle size (between 100-1000 nm)¹⁷. This is mainly attributed to the limited mobility of the in-situ formed surface-active agents that are either amphiphilic copolymers or oligomers consisting of residual groups from initiators with several attached monomer units. During the polymerization, as the surface active agent is generated through the polymerization instead of being readily present in the system at the very beginning, difficulties as coagulation of particles and adhesion to the agitator and reactor walls remain a major challenge in industrial practice. However, in the post-polymerization period, since the stabilizing charges originating in the initiators or functional comonomers are covalently bonded to the particle, the in-situ generated surfactant has less mobility and subsequently less desorption as well as higher surface coverage.³⁹ The combined utilization of ionic initiator and comonomer, and solids content as high as 40% can be obtained by SFEP, although the polydispersity may be higher.⁴⁰

2.3.3 Functional comonomers in SFEP

To increase the latex stability during polymerization, a certain amount of functional comonomers are usually employed in surfactant-free emulsion systems to provide extra stabilizing capability in addition to the initiator residual group located only at the end of the polymer chain. Commonly seen functional monomers in literature can be classified as ionic such as carboxylic monomers,^{41,42} sodium sulfoethyl methacrylate,⁴³ sodium styrene sulfonate,⁴³ sodium undecylenic isethionate,⁴⁴ or non-ionic such as glycidyl methacrylate⁴⁵ and 2-hydroxyethyl methacrylate.⁴⁶ In addition to enhancing colloidal stability, functional comonomers in SFEP have also been increasingly reported to tune the nucleation mechanism. Functional comonomers are usually hydrophilic, and therefore have higher concentration in the continuous phase when copolymerized with hydrophobic monomer such as styrene. At the beginning stages of polymerization, aqueous initiation produces oligomers rich in the functional monomers, which could act as surface active agents in-situ and subsequently aggregate to serve as the precursors of micelles for later particle growth after being swollen with monomers. Although the micellar nucleation mechanism was usually ruled out in SFEP, polymerization carried out with functional monomers is more likely to follow this route. By varying the amount of acrylic acid, Mahdavian and Abdollahi⁴⁷ also concluded that the functional monomer could significantly increase the number of particles and subsequently the overall polymerization rate but it played a minor role in effecting particle growth.

2.4 CO₂-switchable polymers

Carbon dioxide (CO₂) is commonly perceived as the main greenhouse gas caused by incineration of fossil fuels. However, it has increasingly found green applications as a chemical trigger to alter physical or chemical properties of polymers containing CO₂-responsive groups. Responsive behaviors require the assistance of an aqueous environment where CO₂ is dissolved. Amidines, amines and carboxyls are the three most common types of CO₂-responsive groups. Their versatile

applications in CO₂-responsive gels, surfaces, vesicles as well as CO₂ capture materials was recently reviewed by Theato.⁴⁸

2.4.1 CO₂-switchable surface active agent

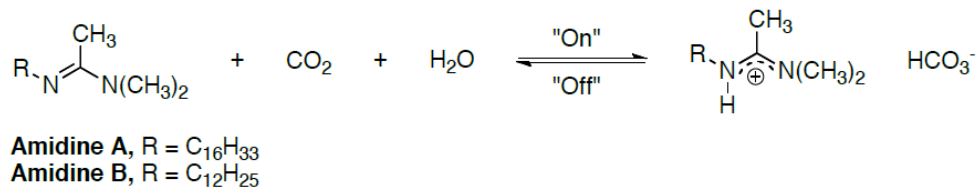
When applied in emulsion polymerization, CO₂-switchable groups can be incorporated by CO₂-switchable surfactants, initiators and comonomers. Compared to conventional triggers such as oxidants, heat or light, responsive systems triggered by CO₂ have illustrated superior advantages in terms of reversibility, low cost, non-requirement of additional chemicals or energy input and environmental compatibility. Table 2.1 summarizes the general application and disadvantages of the existing responsive technologies in emulsion polymerization systems.

Table 2.2 Summary of different types of responsive surfactants

| Technology | Disadvantage | Applications |
|--|---|---|
| Redox-switchable surfactants ^{49,50} | Use of metal-containing or metal-promoted oxidants or reductants, waste generation after each cycle | 1. Fluid thickener; 2. Viscous oil transportation through pipelines; 3. Enhanced oil recovery (EOR); 4. Industrial scale metal equipment degreasing; 5. Textile softeners, conditioning agents, dye-fixing agents, foam stabilizers and corrosion inhibitors. |
| Thermally cleavable surfactants ⁵¹ | Energy-input required for cleavage; one time switch, not reversible | |
| pH-Switchable surfactants ^{52,53} | Addition of acid/base required, salt build up in each cycle | |
| Light-Switchable surfactants ^{54,55} | A very strong light source is required to achieve the switch | |
| Metal-ions Switchable surfactant ⁵⁶ (non-redox) | Complicated peptide synthesis of the surfactant, heavy metal addition | |

For example, a CO₂-switchable surfactant consisting of an amidine group and a long alkyl chain is hydrophobic in its neutral form with poor surface activity. Upon exposure to a CO₂ saturated aqueous phase the amidine group will be protonated as the aqueous pH is lower than its pK_{aH}. It is converted to an effective surfactant as an amphiphilic molecule. The transformation into the charged amidinium bicarbonate, which was noted as the “switching-on” process, can be easily

achieved by simple exposure to one atmosphere CO₂ in an aqueous system and be reversibly “switched-off” by introducing an inert gas (air, N₂ or Ar) into the solution (Scheme 2.1).



Scheme 2.1 Reversible transformation between amidine and its amidinium bicarbonate⁵⁷

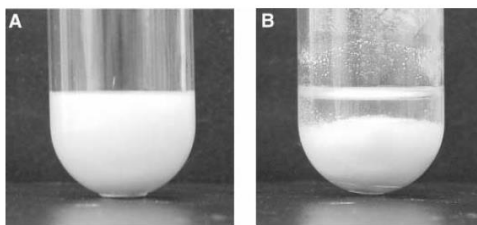


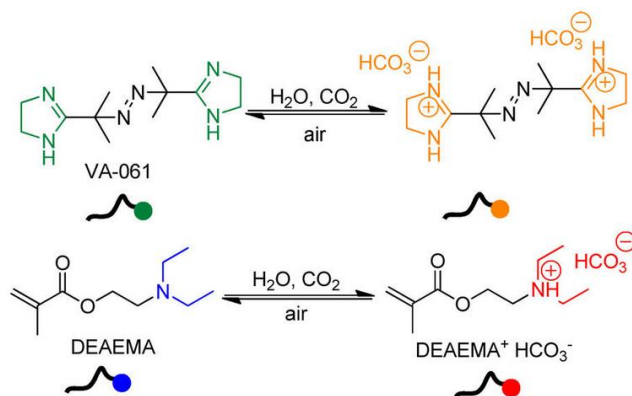
Figure 2.3 Latex stabilized by CO₂-switchable surfactant on(A)/off(B) forms⁵⁷

In an emulsion polymerization system, a CO₂-switchable surfactant can reversibly stabilize and coagulate the colloidal system (Figure 2.3) by alternating between the switched-on and switched-off chemical forms without any further assistant of additional chemicals. A controlled aggregation process is highly industrial desired especially in applications where the end product manufactured by emulsion polymerization is the polymer resin. The current practice to aggregate latex is to add acid/base/salt which will create extra contaminants in the polymer products and require further washing for removal and subsequently creates more waste streams and operational costs. In applications such as coatings, adhesives and paints, where a colloidal form needs to be preserved, the redispersibility may make it possible to store and deliver latex in dry powder or concentrated forms and redisperse it for end uses. The potential cost savings related to

transportation, waste water streams and energy costs has generated increasing interest in industries and driven the academia advances.

The Jessop group has reported the development of several CO₂-switchable components, extending to solvents, solutes, catalysts and even water.⁵⁸ Among them, studies on CO₂-switchable surfactants were successfully employed in emulsion polymerization with styrene⁵⁹ and methyl methacrylate.⁶⁰ The resulting latex was effectively stabilized by the switched-on version of the surfactants and exhibited controlled coagulation by simply expelling CO₂ by purging N₂ or air during post-polymerization process. The latex was then again recovered to its original particle size and zeta-potential by bubbling CO₂ through the solution, commonly accompanied by treatment with sonication. A small library of CO₂-switchable surfactants with designed head groups⁶¹ was developed by the Jessop group. It was found that the basicity (pK_{aH}) of the resulting surfactant bearing certain type of head groups decreased in the order of guanidine >> alkylamidine > imidazolines > N³-arylamidine > 3° amine. The higher basicity promoted the protonation by carbonic acid, which led to more surface active species and correspondingly improved stabilizing performance in emulsion polymerization, while alkylamidine, with its intermediate basicity was more sensitive to the switching-off process at room temperature that promised practical applications.

Su et al.⁶² reported a successful surfactant-free emulsion polymerization using only a CO₂-switchable initiator VA-061 (Scheme 2.2) which could also go through protonation/deprotonation cycles by adding and removing CO₂ into/from the aqueous phase, achieving a CO₂-switchable polystyrene latex with ~7% solids content. Solids content was further increased to ~27%⁶³ by incorporating 0.54% CO₂-responsive comonomer N,N-ethylaminoethyl methacrylate (DEAEMA, Scheme 2.2). Superior colloidal properties were obtained with a monodispersed PDI < 0.054 and small particle size ranging from 230–300 nm.



Scheme 2.2 Protonation/deprotonation of switchable initiator VA-061 and DEAEMA

Preparation of CO₂-switchable latexes by surfactant-free emulsion polymerization will be further explored in this project, focusing on methyl methacrylate systems. By using azo initiators and tertiary amine containing functional comonomers, our goal is to broaden the applicability of CO₂-switchable colloidal technology into relatively hydrophilic monomers. The variation of experimental conditions including monomer feeding ratios, temperature and solids content will be discussed in detail.

References

- (1) Lovell, P. A.; El-Aasser, M. S. *Emulsion Polymerization and Emulsion Polymers*; John Wiley & Sons, Inc., 1997; pp. 60–61.
- (2) Beuermann, S.; Buback, M.; Davis, T. I.; Gilbert, R. G.; Hutchinson, R. A.; Friedrich, O.; Gregory, O. *Macromol. Chem. Phys.* **2006**, *1560*, 1545–1560.
- (3) Davis, T. P.; Matyjaszewski, K. *Hand Book of Radical Polymerization*; John Wiley and Sons, Inc., 2002.
- (4) US Army Chemical Research, D. and E. C. *Review of preparation and properties of polymers from copolymerization of aprotic acrylic monomers with protic acrylic monomers*; 1988; p. 38.
- (5) Miraglia, S. J.; Mayhan, K. G. *J. Appl. Polym. Sci.* **1989**, *38*, 2303–2307.
- (6) Qiu, J.; Charleux, B.; Matyjaszewski, K. *Prog. Polym. Sci.* **2001**, *26*, 2083–2134.
- (7) Chern, C. S. *Prog. Polym. Sci.* **2006**, *31*, 443–486.
- (8) Smith, W. V.; Ewart, R. H. *J. Chem. Phys.* **1948**, *16*, 592–599.
- (9) Harkins, W. D. *J. Am. Chem. Soc.* **1947**, *69*, 1428–1444.
- (10) Priest, W. J. *J. Phys. Chem.* **1952**, *56*, 1077–1082.
- (11) Roe, C. P. *Ind. Eng. Chem.* **1968**, *60*, 20–33.
- (12) Fitch, R. M. *Br. Polym. J.* **1973**, *5*, 467–483.
- (13) Chern, C.-S. *Principles and Application of Emulsion Polymerization*; John Wiley & Sons, Inc., 2008; pp. 12–13.
- (14) Verwey E. J. W.; Overbeek J. Th. G. *Theory of the Stability of Lyophobic Colloids*; Elsevier Ltd, 1948; p. 4.
- (15) Paul C. Hiemenz, Raj Rajagopalan. *Principles of colloid and surface chemistry*; 3rd ed.; 1997.
- (16) Robert G. Gilbert. *Emulsion polymerization: a mechanistic approach*; Academic Press, 1995.
- (17) Arshady, R. *Colloid Polym. Sci.* **1992**, *270*, 717–732.
- (18) Chu, H.; Hwang, H. *Polym. Bull.* **1997**, *302*, 295–302.

- (19) Ramos, J.; Forcada, J. *Eur. Polym. J.* **2007**, *43*, 4647–4661.
- (20) Fitch, R. M.; Watson, R. C. *J. Colloid Interface Sci.* **1979**, *68*, 14–20.
- (21) Zimehl, R.; Lagaly, G.; Ahrens, J. *Colloid Polym. Sci.* **1990**, *268*, 924–933.
- (22) Song, Z.; Poehlein, G. W. *J. Colloid Interface Sci.* **1989**, *128*, 486–500.
- (23) Bagchi, P.; Gray, B. .; Birnbaum, S. . *J. Colloid Interface Sci.* **1979**, *69*, 502–528.
- (24) Gardon, J. L. *J. Phys. Chem. A* **1968**, *6*, 643–664.
- (25) Ou, J.; Yang, J.; Chen, H. *Eur. Polym. J.* **2001**, *37*, 789–799.
- (26) Camli, S. T.; Buyukserin, F.; Balci, O.; Budak, G. G. *J. Colloid Interface Sci.* **2010**, *344*, 528–532.
- (27) Chu, X.; Wasan, D. *J. Colloid Interface Sci.* **1996**, *184*, 268–278.
- (28) T. Matsumoto and A. Ochi, K. K. *Chem. High Polym.* **1965**, *22*, 481–487.
- (29) Fitch, R. M.; Prenosil, M. B.; Sprick, K. J. *J. Polym. Sci. Part C Polym. Symp.* **2007**, *27*, 95–118.
- (30) Goodwin, J. W.; Hearnb, J.; Hoe, C. C.; Ottewill, R. H. *Br. Polym. J.* **1973**, *5*, 347–362.
- (31) Hansen, F. K.; Ugelstad, J. *J. Polym. Sci. Polym. Chem. Ed.* **1978**, *16*, 1953–1979.
- (32) Feeney, P. J.; Napper, D. H.; Gilbert, R. G. *Macromolecules* **1987**, *20*, 2922–2930.
- (33) Wang, Y.; Pan, C. Y. *Colloid Polym. Sci.* **1999**, *665*, 658–665.
- (34) Hansen, F. K.; Ugelstad, J. *J. Polym. Sci. Polym. Chem. Ed.* **1979**, *17*, 3047–3067.
- (35) Goodwin, J. W.; Ottewill, R. H.; Pelton, R.; Vianello, G.; Yates, D. E. *Br. Polym. J.* **1978**, *10*, 173–180.
- (36) Ramos, J.; Forcada, J. *Eur. Polym. J.* **2010**, *46*, 1106–1110.
- (37) Alexandridis, P. *Curr. Opin. Colloid Interface Sci.* **1996**, *1*, 490–501.
- (38) Dai, S.; Ravi, P.; Tam, K. C. *Soft Matter* **2008**, *4*, 435–449.
- (39) Ceska, G. W. *J. Appl. Polym. Sci.* **1974**, *18*, 427–437.
- (40) Bourgeat-Lami, E.; Guimarães, T. R.; Pereira, A. M. C.; Alves, G. M.; Moreira, J. C.; Putaux, J.-L.; Dos Santos, A. M. *Macromol. Rapid Commun.* **2010**, *31*, 1874–1880.

- (41) Ceska, G. W. *J. Appl. Polym. Sci.* **1974**, *18*, 2493–2499.
- (42) Sakota, K.; Okaya, T. *J. Appl. Polym. Sci.* **1976**, *20*, 1725–1733.
- (43) Juang, M. S.-D.; Krieger, I. M. *J. Polym. Sci. Polym. Chem. Ed.* **1976**, *14*, 2089–2107.
- (44) Chen, S.; Chang, H. *J. Polym. Sci. Polym. Chem. Ed.* **1985**, *23*, 2615–2630.
- (45) Žůrková, E.; Bouchal, K.; Zdeňková, D.; Pelzbauer, Z.; Švec, F.; Kálal, J.; Batz, H. G. *J. Polym. Sci. Polym. Chem. Ed.* **1983**, *21*, 2949–2960.
- (46) Kamei, S.; Okubo, M.; Matsumoto, T. *J. Polym. Sci. Part A Polym. Chem.* **1986**, *24*, 3109–3116.
- (47) Mahdavian, A.-R.; Abdollahi, M. *Polymer (Guildf)*. **2004**, *45*, 3233–3239.
- (48) Lin, S.; Theato, P. *Macromol. Rapid Commun.* **2013**, *34*, 1118–1133.
- (49) Datwani, S. S.; Nguyen Truskett, V.; Rosslee, C. A.; Abbott, N. L.; Stebe, K. J. *Langmuir* **2003**, *19*, 8292–8301.
- (50) Cheng, Z.; Ren, B.; Gao, M.; Liu, X.; Tong, Z. *Macromolecules* **2007**, *40*, 7638–7643.
- (51) McElhanon, J. R. Thermally cleavable surfactants. US 7,022,861 B1, 2004.
- (52) Minkenberg, C. B.; Florusse, L.; Eelkema, R.; Koper, G. J. M.; van Esch, J. H. *J. Am. Chem. Soc.* **2009**, *131*, 11274–11275.
- (53) Malcolm, A. S.; Dexter, A. F.; Middelberg, A. P. J. *Soft Matter* **2006**, *2*, 1057–1066.
- (54) Mirarefi, P.; Lee, C. T. *Biochim. Biophys. Acta* **2010**, *1804*, 106–114.
- (55) Sakai, H.; Matsumura, A.; Yokoyama, S.; Saji, T.; Abe, M. *J. Phys. Chem. B* **1999**, *103*, 10737–10740.
- (56) Dexter, a. F.; Middelberg, a. P. J. *J. Phys. Chem. C* **2007**, *111*, 10484–10492.
- (57) Liu, Y.; Jessop, P. G.; Cunningham, M.; Eckert, C. A.; Liotta, C. L. *Science* **2006**, *313*, 958–960.
- (58) Jessop, P. G.; Mercer, S. M.; Heldebrant, D. J. *Energy Environ. Sci.* **2012**, *5*, 7240–7253.
- (59) Mihara, M.; Jessop, P.; Cunningham, M. *Macromolecules* **2011**, *44*, 3688–3693.
- (60) Fowler, C. I.; Muchemu, C. M.; Miller, R. E.; Phan, L.; O'Neill, C.; Jessop, P. G.; Cunningham, M. F. *Macromolecules* **2011**, *44*, 2501–2509.
- (61) Scott, L. M.; Robert, T.; Harjani, J. R.; Jessop, P. G. *RSC Adv.* **2012**, *2*, 4925–4931.

- (62) Su, X.; Jessop, P. G.; Cunningham, M. F. *Macromolecules* **2012**, *45*, 666–670.
- (63) Pinaud, J.; Kowal, E.; Cunningham, M.; Jessop, P. *ACS Macro Lett.* **2012**, *1*, 1103–1107.

Chapter 3

CO₂-Switchable PMMA Latexes with Controllable Particle Size

Prepared by Surfactant-Free Emulsion Polymerization

Abstract CO₂-switchable poly(methyl methacrylate) (PMMA) latexes were prepared by surfactant-free emulsion polymerization using the initiator 2,2'-azobis[2-(2-imidazolin-2-yl)propane]dihydrochloride (VA-044) and a small fraction of functional comonomer N,N-dimethylaminoethyl methacrylate (DMAEMA). The latexes demonstrated superior CO₂ responsive behavior with rapid aggregation, and with a complete recovery of particle size and polydispersity upon redispersion without requiring high energy mixing and within a short period of time. Particle size was successfully tuned in a range of 170~500 nm by varying the ratio of VA-044:DMAEMA, total amount of stabilizing moieties (VA-044+DMAEMA), temperature and solids content. Both particle size and CO₂-switchable performance were closely related to the ratio of VA-044:DMAEMA, with the ratio of VA-044:DMAEMA=1:3 yielding both the smallest particle size and the most efficient CO₂ responsiveness.

3.1 Introduction

Surfactant-free emulsion polymerization (SFEP) has gained increasing interest in both academia and industry for its ability to produce nanoparticles in the absence of added surfactant. In SFEP the particle size is controlled by the concentration of species that act as stabilizing moieties, as compared to conventional emulsion polymerization where added surfactant plays a leading role in determining latex properties.

N,N-Diethylaminoethyl methacrylate (DEAEMA) and N,N-dimethylaminoethyl methacrylate (DMAEMA) are tertiary amine containing monomers that exhibit CO₂ responsiveness. Their polymers have pK_{aH} values of 7.5 and 7.4 respectively.¹ After Jessop and coworkers² reported the first CO₂-switchable surfactant, DMAEMA and DEAEMA were adopted as CO₂-responsive agents³⁻⁶ in emulsion systems. Zhu's⁷ group pre-synthesized a block copolymer of PMMA-b-PDMAEMA as a surfactant that was subsequently used in preparing PMMA latex via emulsion polymerization. A further investigation was carried out by the same group to look into the relationship between the composition of the block copolymer and its performance as a surfactant in terms of stabilizing PMMA latexes.⁸ In both studies, the polymeric surfactant that contained different amounts of DMAEMA units was first protonated by HCl (~pH 3) in order to conduct the emulsion polymerization. Sodium hydroxide (NaOH) was used in the first switching-off cycle to aggregate the latex. Redispersion/aggregation (switching-on/off) cycles of the latex could then be performed by purging CO₂ or N₂ due to the change of hydrophobicity/hydrophilicity of DMAEMA tertiary amine units. The authors also noted a failed attempt to carry out the same experiment under a CO₂ environment. Our group successfully prepared CO₂-switchable polystyrene (PS) latex via surfactant-free emulsion polymerization.⁹ Excellent colloidal properties (particle size <300nm, PDI<0.05) as well as CO₂-switchability were both achieved by combining the use of CO₂-responsive initiator VA-061 as well as a small amount (0.54%) of DEAEMA as comonomer

under a CO₂ environment. PDEAEMA oligomer was proposed to act as a flocculant, promoting coagulation upon N₂ introduction.

One of the major unsolved challenges for CO₂-switchable latexes is the necessity of sonication for redispersion for both latexes prepared using a pre-made CO₂-switchable surfactant^{2,10-12} or for latexes stabilized by initiator¹³ or the combination of initiator and comonomer.¹⁴ Sonication is highly energy intensive and not feasible in large scale industrial processes. In this study we have prepared CO₂-switchable PMMA latexes using surfactant-free emulsion polymerization. Stabilization is provided by tertiary amine containing groups in the comonomer DMAEMA and amidine groups in the initiator. The latexes can be rapidly and effectively aggregated and redispersed. Redispersion can be achieved without sonication or high energy mixing.

3.2 Experimental Methods

3.2.1 Materials

Hydrochloric acid (HCl, Aldrich), deuterated water (D₂O, Cambridge Isotope Laborites) 2,2'-azobis[2-(2-imidazolin-2-yl)propane]dihydrochloride (VA-044, Wako), sodium chloride (NaCl, Sigma-Aldrich, >99%), sodium hydroxide (NaOH, Sigma-Aldrich, >98%), carbon dioxide (CO₂, Praxair, Medical Degree) and nitrogen (N₂, Praxair, Ultra High Purity, 5.0) were used as received. Monomers N,N-dimethylaminoethyl methacrylate (DMAEMA, Aldrich, 99%) and methyl methacrylate (MMA, Aldrich, 99%) were purified by inhibitor removal columns. Distilled and deionized water used for all experiments was purified through a Synergy iron exchange unit supplied by Millipore.

3.2.2 Surfactant-free emulsion polymerization using VA-044 and DMAEMA

Emulsion polymerizations were conducted in a six-well carousel reactor (Radley's Innovation Technology). Distilled water (45 ml) was first added into a flask together with DMAEMA, followed by dropwise addition of one mole equivalent of HCl (1 M) to DMAEMA. The mixture

was left stirring for 15 min. The flasks were then fit onto the carousel reactor for pre-heating with constant N₂ bubbling for 30 min. VA-044 was weighed into 20 ml scintillation vials with 5 ml water and purged with N₂ in an ice bath until completely dissolved. Pre-purged MMA was injected into the flasks followed by initiator solution to start the reaction. N₂ purging was continued for another 5 min before the flasks were sealed to avoid monomer evaporation during reaction. All experiments were run for 1 hour. Samples were withdrawn periodically for DLS analysis and conversion determination.

3.2.3 Coagulation and redispersion of latex

The first cycle of switching on and off was conducted using an NaOH solution (1 M). NaOH was added dropwise into 8 g of latex until the pH stabilized in the range of 9.5~10.1. The mixture was left stirring for 20 min prior to centrifuging at 3000 rpm for 1 min. The sediment was collected and the supernatant was replaced by fresh distilled water until the total weight reached the original 8 g, with 3 g set aside for characterization. The remaining 5 g was purged by CO₂ in a capped vial for 5 min at room temperature (mechanical stirring was not applied.) The redispersed latex was then treated with N₂ in a 60°C water bath until visible precipitation (within 5 min) for a second cycle of coagulation, followed by another 5 min CO₂ bubbling at room temperature for redispersion. Particle size and zeta-potential were monitored after each procedure on either the Zetasizer Nano(redispersed) or Mastersizer (coagulated). Samples that could not be successfully aggregated or redispersed in the first cycle were not carried on to the second switching cycle.

3.2.4 Characterization

Monomer conversions were determined gravimetrically. 2-4 ml samples were withdrawn and cooled immediately in an ice bath to stop further polymerization. Samples were first dried under air flow overnight at room temperature and in a vacuum oven for another 12 hours. Conversion was calculated as follows:

$$\text{conversion} = \frac{(M_{\text{dry}})(M_{\text{MMA}} + M_{\text{DMAEMA}} + M_{\text{I}} + M_{\text{water}})}{M_{\text{wet}}(M_{\text{MMA}} + M_{\text{DMAEMA}} + M_{\text{I}})} \quad (3.1)$$

Where M_{MMA} , M_{DMAEMA} , M_{I} , M_{water} are the mass of MMA, DMAEMA⁺Cl⁻, initiator and water, respectively; and M_{dry} , M_{wet} is the mass of the latex sample and the mass of the dried polymer.

Number of particles was calculated by Equation 3.2,

$$N_p = \frac{6P_p}{\rho_p \pi d_z^3} \times 1000/L \quad (3.2)$$

Where ρ_p = density of the polymer, (g/cm³)

d_z = diameter of the particle, (nm, intensity value obtained from Malvern Zetasizer Nano ZS)

P_p = grams of the polymer per cm³ of water (g/cm³water)

and P_p was further determined by Equation 3.3,

$$P_p = \frac{\text{Monomer}(g) \times \text{conversion}}{\text{Water}(cm^3) \times 100} \quad (3.3)$$

Where weight of monomer was the initial amount of monomer added into the system before polymerization.

Total stabilized surface Area (A) was calculated by Equation 3.4,

$$A = 4\pi \left(\frac{d_z}{2}\right)^2 \times N_p \quad (3.4)$$

Particle size and zeta-potential were measured on a Malvern Zetasizer Nano ZS (size range 0.3 nm to 10 μ m) at 25°C and an angle of 173° using a disposable capillary cuvette and a universal dip cell (DTS1070) for zeta-potential. Samples were diluted with distilled water for the original latex and with CO₂ saturated water for those redispersed by CO₂ protonation prior to measurement. Dilution was precisely controlled by 10 μ l latex vs. 2 ml water for 10% solids

content entries and proportionally adjusted for 5%, 15% and 20% solids content entries in order to avoid instrumental variations on particle size caused by sample concentration. Reported intensity-average values were taken as an average of 3 measurements with 13 runs each. Particle size after destabilization was determined using a Malvern Mastersizer 2000 (size range of 50 nm to 2000 μm) equipped with a Hydro2000S optical unit. The refractive index of the copolymer was approximated by that of PMMA on both instruments. A Thermo Scientific Orion Star A215 calibrated with aqueous standards (pH 4, 7, and 10) was used to measure pH. Molecular weight and polydispersity (PDI) of the polymer were measured using Waters 2690 Separation Module and Waters 410 Differential Refractometer with THF as the eluent at a flow rate of 0.3 mL \cdot min $^{-1}$. The column bank consisted of Waters Styragel HR (4.6x300 mm) 4, 3, 1, and 0.5 separation columns coupled with a Waters 410 differential refractive index detector calibrated with poly(methyl methacrylate) standards ranging from 1020 to 853,000 g \cdot mol $^{-1}$ at 40°C. Dry polymer samples were first dispersed in THF followed by neutralization of equivalent amount of NaOH (1M), sonicated for half an hour, dried and redissolved in THF.

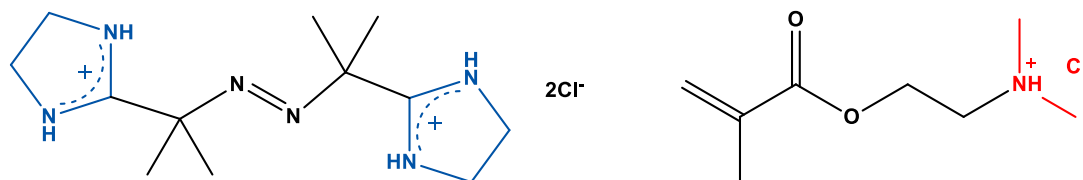
3.3 Results and discussions

3.3.1 Surfactant-free emulsion polymerization of methyl methacrylate

DMAEMA has a 5% water solubility at 20°C¹⁵ with basic pH of its aqueous solution. It was reported that DMAEMA would undergo fast hydrolysis in a basic aqueous phase ($t_{1/2}$ =3.31 h at pH 9, 25°C),¹⁶ which could be efficiently prevented by sufficient protonation (stable at pH 4, 50 °C).¹⁶ Therefore, in all experimental entries, DMAEMA was first protonated by one equivalent of HCl (1 M) before polymerization to minimize hydrolysis. The pH of the resulting neutralized solution was usually between 6~7 depending on the amount of chloride salt of DMAEMA. Excessive acid addition was avoided to prevent the influence of the increased ionic strength on particle size and latex stability. Protonation also brought the benefit of increased solubility and

made DMAEMA a more hydrophilic comonomer. The higher water solubility would enable more DMAEMA units to be located on the particle surface and increase stabilization.

Initiator VA-044 is an azo initiator with fast decomposition kinetics having a 10 hour half-life temperature at 44 °C in water.¹⁷ The cationic imidazole ring provides an electrostatic stabilizing force as a residual group of the initiator attached to the end of the polymer chains. The protonated functional comonomer DMAEMA⁺Cl⁻ was the other source of positive charge, also originating in the cationic nitrogen atom (Scheme 3.1).



Scheme 3.1 Structures of VA-044 (left) and protonated DMAEMA (right)

3.3.1.1 Effect of VA-044:DMAEMA ratio on latex properties

The first set of polymerizations (N-series) was carried out with a constant functional group concentration (N⁺%) in order to examine the effect of each type of stabilizing moiety on the final latex properties.

$$C_{\text{functional group}} (\text{N}^+\%) = C_{\text{VA-044}} \times 2 + C_{\text{DMAEMA}} = C_{\text{MMA}} \times 2\% \quad (3.5)$$

Where $C_{\text{functional group}}$ is the concentration of overall functional groups, $C_{\text{VA-044}}$, C_{DMAEMA} , and C_{MMA} are the concentrations of VA-044, DMAEMA and MMA, respectively.

Theoretically, a fixed concentration of charged groups might be expected to provide the same level of stabilizing capacity, and stabilize the same amount of overall surface area. Therefore,

with a constant amount of monomer, the resulting number of particles as well as the final particle size should be similar.

Table 3.1 SFEP recipe and latex properties with constant concentration of overall functional groups at 65 °C

| EXP | MMA | H ₂ O | VA-044 | DMAEMA | Size | PDI | Zeta | Conv. | N _p |
|------|-----|------------------|--------------------|--------------------|------|-------|-------|-------|------------------------|
| | /ml | /ml | /mol% ^a | /mol% ^a | /nm | | /mV | /% | /(10 ¹⁶ /L) |
| N-1 | 6 | 50 | 0.1 | 1.8 | 335 | 0.073 | +64.4 | 99 | 0.50 |
| N-5 | 6 | 50 | 0.2 | 1.6 | 283 | 0.020 | +58.2 | 98 | 0.82 |
| N-6 | 6 | 50 | 0.3 | 1.4 | 268 | 0.016 | +54.9 | 99 | 0.96 |
| N-2 | 6 | 50 | 0.4 | 1.2 | 249 | 0.021 | +54.1 | 95 | 1.16 |
| N-7 | 6 | 50 | 0.5 | 1 | 267 | 0.035 | +55.3 | 99 | 0.97 |
| N-8 | 6 | 50 | 0.6 | 0.8 | 288 | 0.046 | +54.3 | 99 | 0.77 |
| N-3 | 6 | 50 | 0.7 | 0.6 | 289 | 0.097 | +52.2 | 99 | 0.76 |
| N-9 | 6 | 50 | 0.8 | 0.4 | 319 | 0.069 | +58.3 | 100 | 0.58 |
| N-10 | 6 | 50 | 0.9 | 0.2 | 321 | 0.095 | +52.9 | 98 | 0.55 |
| N-4 | 6 | 50 | 1 | 0 | 387 | 0.136 | +50.2 | 98 | 0.31 |

As illustrated in Table 3.1, the percentage of VA-044 was varied from 0.1 mol% to 1 mol% with the added amount of DMAEMA correspondingly adjusted from 1.8 mol% to 0 mol%, at a constant solids content of ~10%. Experiments were carried out at 65°C for an hour, with high conversions achieved in nearly all runs. The resulting latex demonstrated high zeta-potential (above +50 mV), indicating superior colloidal stability. With an increased portion of VA-044 among the total charged species, zeta-potential decreased slightly, from above +55 mV with 0.1~0.4 mol% initiator addition compared to that of the generally below +55 mV with 0.5~1 mol%

addition. This was mainly attributed to the fact that the initiation efficiency of VA-044 was not 100% and thus positive groups from the initiator were not entirely incorporated into the polymer chains. The contribution of VA-044 to the charged population on the particle surface was therefore diminished. This was confirmed by GPC results showing an average initiation efficiency of ~0.3 (Table 3.2), under the assumption that termination occurred by combination.^{18,19}

The initiation efficiency (f) was calculated according to Equation 3.6,

$$f = \frac{M_{MMA}}{(VA-044 \text{ mol}\%) \times M_{n/GPC}} \quad (3.6)$$

Where VA-044 mol% is the mole percent of initiator VA-044 with respect to MMA, and $M_{n/GPC}$ is the number average molecular weight obtained from GPC. The mole mass of MMA, M_{MMA} , is 100.12 g/mol.

Table 3.2 GPC results of N-Series on molecular weight, PDI and initiation efficiency

| Entry | N-1 | N-5 | N-6 | N-2 | N-7 | N-8 | N-3 | N-9 | N-10 | N-4 | Ave. |
|------------|-------|-------|-------|-------|------|--------|--------|--------|--------|------|------|
| V:D | 1:9 | 1:4 | 1:2.3 | 1:1.5 | 1:1 | 1:0.67 | 1:0.43 | 1:0.25 | 1:0.11 | 1:0 | - |
| $M_n/10^3$ | 212.2 | 176.1 | 139.1 | 135.1 | 70.5 | 49.3 | 46.5 | 41.2 | 36.2 | 31.9 | - |
| PDI | 1.63 | 1.64 | 1.72 | 1.75 | 1.96 | 2.44 | 2.39 | 2.74 | 2.46 | 2.5 | - |
| f | 0.47 | 0.28 | 0.24 | 0.19 | 0.28 | 0.34 | 0.31 | 0.30 | 0.31 | 0.31 | 0.30 |

*V:D=VA-044:DMAEMA(mol:mol)

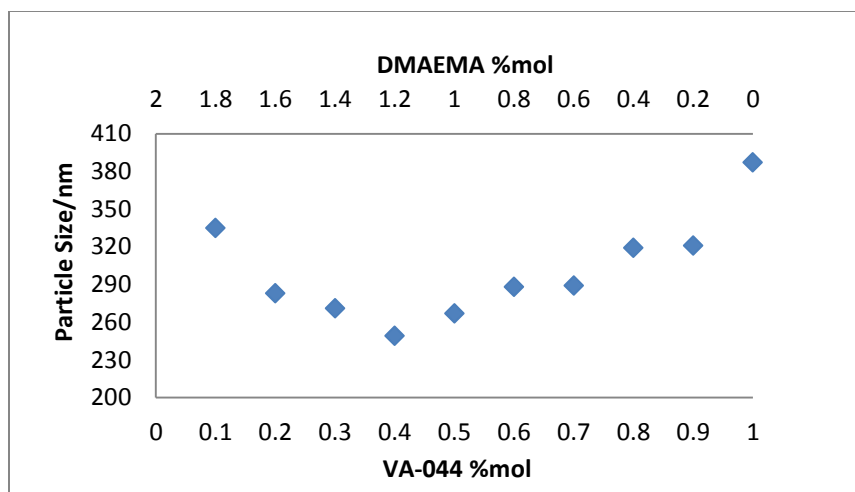


Figure 3.1 Particle size versus VA-044 mol% / DMAEMA mol% with fixed total N^+ at 2 mol%

Particle size experienced a V-shape evolution with increasing amount of VA-044 and decreasing amount of DMAEMA (Figure 3.1), with a decreasing trend until 0.4% VA-044 (N-2) to reach the smallest particle size at 249 nm and then increasing to 387 nm at 1% VA-044. Using only VA-044 (in the absence of DMAEMA) (N-4) gave the largest particle size indicating that stabilizing capacity provided by the initiator residual groups alone was rather limited. This was further confirmed by the calculation of total stabilized surface area (Figure 3.2) where N-4 also gave the smallest value. As previously mentioned, the relatively poor initiation efficiency at ~ 0.3 would lead to 70% loss of stabilization capability from the initiator. When the proportion of initiator increased, the overall amount of stabilizing species was decreasing. Particle size was larger at higher VA-044 concentration within the range of VA-044 addition 0.4%~1%. The location the VA-044 derived charges were only at the polymer chain end and this may be another cause of the less efficient stabilization. As VA-044 was gradually replaced by small amounts of DMAEMA from 0% to 1.2%, the particle size underwent a continuous drop with accompanying increasing particle surface area. This was a reflection of enhanced stabilization and suggested that within the given VA-044 concentration range, randomly distributed DMAEMA⁺ groups along the polymer chain could act as a more efficient in-situ generated surface active agent compared to VA-044.

Particle size started to increase as more VA-044 was replaced by DMAEMA in the range of 0.1% ~ 0.4% VA-044 addition. Low concentration of VA-044 limited the initiation process and subsequently limited the nucleation. Particle generation requires that there are a sufficient amount of polymer (oligomer) chains present in the continuous phase. Therefore, initiation became the limiting step in this VA-044 concentration range. Particle size decreased with increasing amount of initiation as more aqueous oligoradicals were generated and hence more particles were nucleated (Figure 3.2). When there were adequate numbers of primary particles present in the continuous phase, the newly initiated radicals or oligomers were more likely to enter these particles instead of creating new particles.

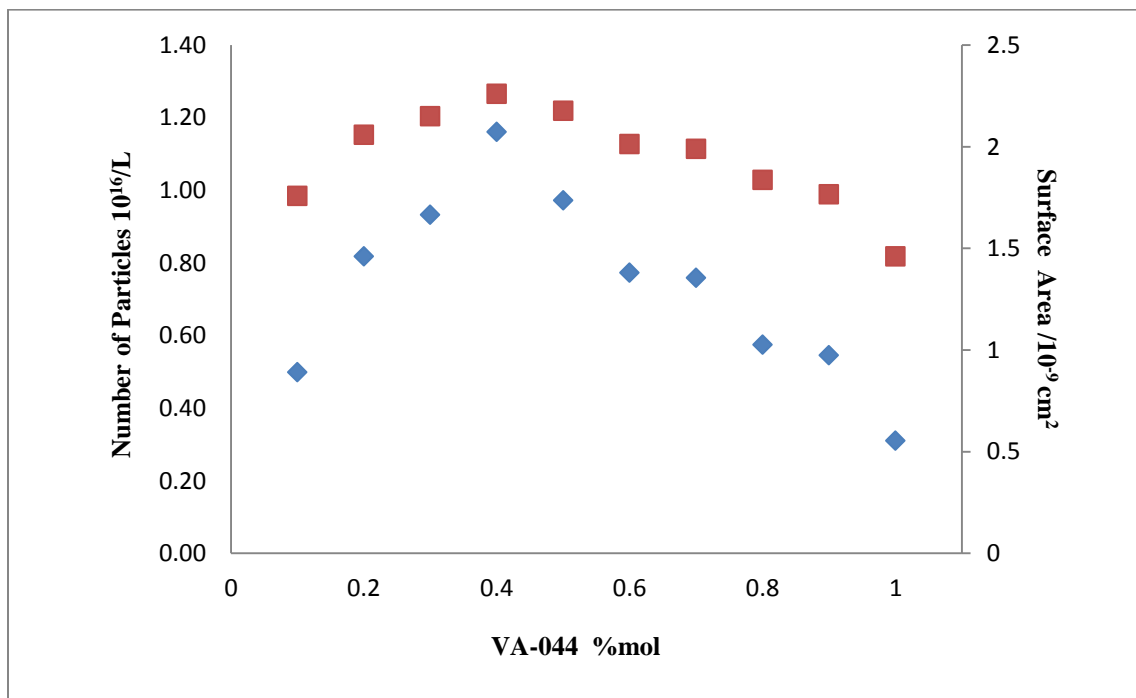


Figure 3.2 Number of particles and total stabilized surface area with increasing percentage of VA-044 at fixed number of total N^+ (2 mol%)

To further understand the role of DMAEMA⁺, experiments with 0.1%, 0.4%, 0.7% and 1% VA-044 were carried out at a reduced temperature of 55 °C to slow down the kinetics and prolong the nucleation stage. Conversion at the early stages of polymerization was closely monitored at the first 20 min by sampling every 5 min. Figure 3.3 clearly demonstrates that higher concentration of initiator led to a faster monomer conversion. GPC results also showed that the average molecular weight was inversely related to the amount of initiator, indicating the total number of polymer chains was increased with increasing VA-044. The disagreement of trends in number of polymer chains and the number of polymer particles further proved that nucleation was not entirely dependent on the initiation and that VA-044 alone has limited capability at tuning the number of particles.

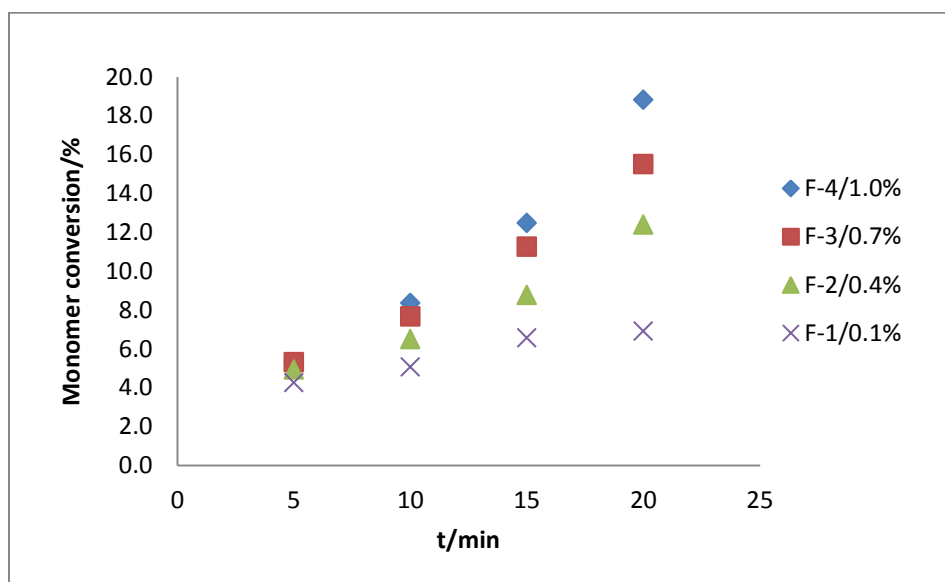


Figure 3.3 Monomer conversion versus time at the early stages of polymerization at 55 °C with initiator concentrations at 0.1 mol% (F-1), 0.4 mol% (F-2), 0.7 mol% (F-3) and 1.0 mol% (F-4)

To summarize, at a given temperature and monomer concentration in our SFEP system, both types of charged species from the initiator residual groups and the protonated DMAEMA

participated in the nucleation process. The concentration of VA-044 influences the rate of polymerization at the beginning stage by initiating polymer chains and enhances particle nucleation by initiating more polymer chains up to ~0.4 mol%.

In order to exclude the possible influence on the particle size of increased initial ionic strength with increasing amount of VA-044, experiment series N-P was conducted with ionic strength maintained constant by NaCl (1 M) addition. N-4 (entry with highest initial ionic strength) was chosen as the reference condition. Particle size increased slightly upon extra salt addition as expected, mainly attributed to the reduced thickness of the electrostatic double layer. However, the same trend observed earlier was preserved. The initial ionic strength and the amount of added NaCl were calculated according to Equations 3.7 and 3.8, respectively.

$$I = 3 \times C_{VA-044} + C_{HCl} \quad (3.7)$$

$$C_{NaCl} = I_{N-4} - I_{N-Pi} \quad (3.8)$$

Where I is the initial ionic strength, C_{NaCl} is the concentration of NaCl added, and i is the entry number in experiment series N-P.

Table 3.3 SFEP recipe and latex properties with calibrated ionic strength at 65 °C

| EXP | NaCl(1M) /ml | VA-044 /mol% ^a | DMAEMA /mol% ^a | Size /nm | PDI | Zeta /mV | Conv. /% | N_p /(10 ¹⁶ /L) |
|-------|-----------------|------------------------------|------------------------------|-------------|-------|-------------|-------------|---------------------------------|
| N-P-1 | 0.504 | 0.2 | 0.6 | 511 | 0.12 | +48.3 | 99 | 0.14 |
| N-P-2 | 0.336 | 0.4 | 1.2 | 286 | 0.006 | +48.4 | 99 | 0.78 |
| N-P-3 | 0.168 | 0.6 | 1.8 | 289 | 0.004 | +47.4 | 100 | 0.76 |
| N-4 | 0 | 0.8 | 2.4 | 387 | 0.136 | +50.2 | 98 | 0.31 |

General recipe used: MMA/H₂O=6 ml/50 ml

3.3.1.2 Effects of varying the overall amount of stabilizing force

Experiment series O and series I were carried out with the purpose of exploring the effects of overall amount of added stabilizers (DMAEMA+VA-044) on the final latex particle size, in an effort to reduce the overall amount of charged species while maintaining relatively small particle

size and narrow polydispersity. In industrial applications, less initiator and/or comonomer addition means lower cost and higher product purity including lower moisture sensitivity. A negative correlation should be expected between the concentration of overall functional groups and the final particle size. We chose N-2 as the reference case, with VA-044:DMAEMA ratio at 1:3 under fixed concentration of overall functional groups (2 mol% with respect to MMA). In series O, the VA-044/DMAEMA ratio was kept constant at 1:3 while the concentration of overall functional groups with respect to MMA was varied from 1 mol% to 4 mol%. In series I, the amount of initiator was kept constant at 0.4 mol%, and addition of DMEAMA was varied to both the lower end (0.6 mol%) and higher end (2.4 mol%.)

Table 3.4 SFEP recipe and latex properties with fixed V:D ratio (1:3) with varied overall N⁺%

| EXP | MMA /ml | H ₂ O /ml | VA-044 /mol% ^a | DMAEMA /mol% ^a | Size /nm | PDI | Zeta /mV | Conv. /% | N _p /(10 ¹⁶ /L) |
|-----|------------|-------------------------|------------------------------|------------------------------|-------------|-------|-------------|-------------|--|
| O-3 | 6 | 50 | 0.2 | 0.6 | 285 | 0.020 | +57.5 | 99 | 0.79 |
| N-2 | 6 | 50 | 0.4 | 1.2 | 249 | 0.021 | +54.1 | 95 | 1.16 |
| O-1 | 6 | 50 | 0.6 | 1.8 | 277 | 0.062 | +54.0 | 98 | 0.88 |
| O-2 | 6 | 50 | 0.8 | 2.4 | 238 | 0.017 | +51.9 | 99 | 1.41 |

Table 3.5 SFEP recipe and latex properties with varied amount of DMAEMA at 65 °C
at constant VA-044 addition (0.4 mol%)

| EXP | MMA /ml | H ₂ O /ml | VA-044 /mol% ^a | DMAEMA /mol% ^a | Size /nm | PDI | Zeta /mV | Conv. /% | N _p /(10 ¹⁶ /L) |
|-----|------------|-------------------------|------------------------------|------------------------------|-------------|-------|-------------|-------------|--|
| I-1 | 6 | 50 | 0.4 | 0.6 | 292 | 0.017 | +49 | 100 | 0.76 |
| N-2 | 6 | 50 | 0.4 | 1.2 | 249 | 0.021 | +54.1 | 95 | 1.16 |
| I-2 | 6 | 50 | 0.4 | 1.8 | 273 | 0.022 | +49.2 | 100 | 0.93 |
| I-3 | 6 | 50 | 0.4 | 2.4 | 257 | 0.017 | +50.3 | 100 | 1.13 |

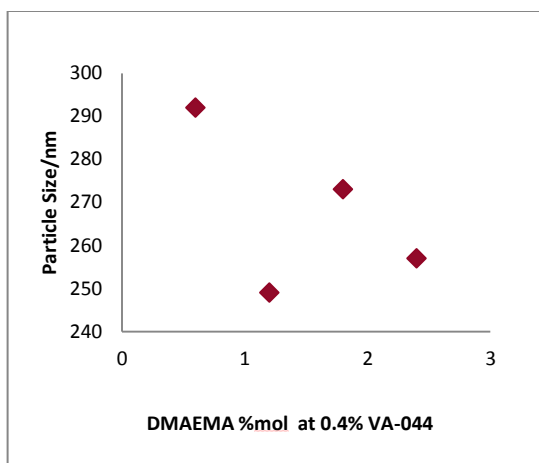


Figure 3.4 Particle size versus total N⁺% at constant V:D ratio 1:3 (Series O)

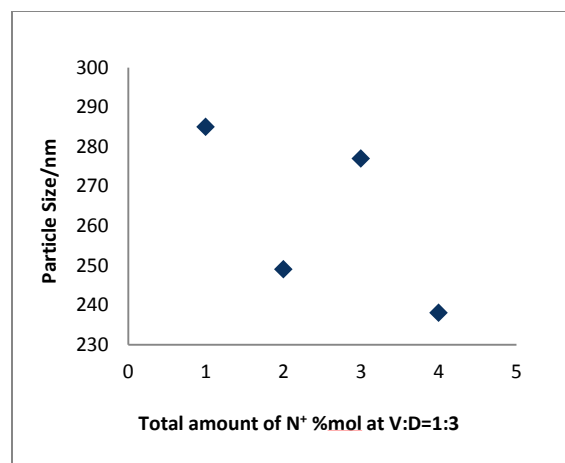


Figure 3.5 Particle size versus concentration of DMAEMA at constant VA-044 level (Series I)

In series O, particle size (compared to N-2 at 249 nm) increased to 285 nm when the total N⁺% decreased from 2% to 1% that was mostly due to the reduced availability of surface active agents. However, when the total N⁺% increased to 3%, the particle size also increased slightly followed by a decrease at 4% addition of total N⁺%. The same trend was observed in Series I. At a constant initiator level (as compared to N-2), decreasing the amount of DMAEMA led to slightly larger particle diameter while gradual increase of DMAEMA did not always produce smaller particles. For example, I-3 with 1.2mol% DMAEMA (compared to N-2 (0.6 mol%)) yielded larger particles. The difference in trend compared to Series O was that a continuing increase in DMAEMA (2.4 mol%) did not reduce the particle size to a diameter that was smaller than N-2 (1.2 mol%), although it was smaller than I-2 (1.8 mol%). Similar behaviour was previously reported by Wu²⁰ and coworkers during the study of the dual role of KPS of stabilizing/destabilizing an SFEP system, where the hydrodynamic radius first decreased with the increased amount of KPS and then increased as the addition continued. The most possible cause was that VA-044 and DMAEMA⁺ as well as their counterion Cl⁻ in the aqueous phase contributed

to the initial total ionic strength. This behaviour was also experimentally observed in the N-P series.

Within the concentration range investigated, there was a pair of effects competing to determine the final particle size with increasing total N^+ %. While increased total stabilizing force contributed to smaller particle diameter, the accompanying higher ionic strength tended to increase it. The resulting latex would have a particle size as a combined result of these two effects. Therefore, excessive addition of either initiator or DMAEMA was not necessarily favourable to produce smaller particle size or superior colloidal stability.

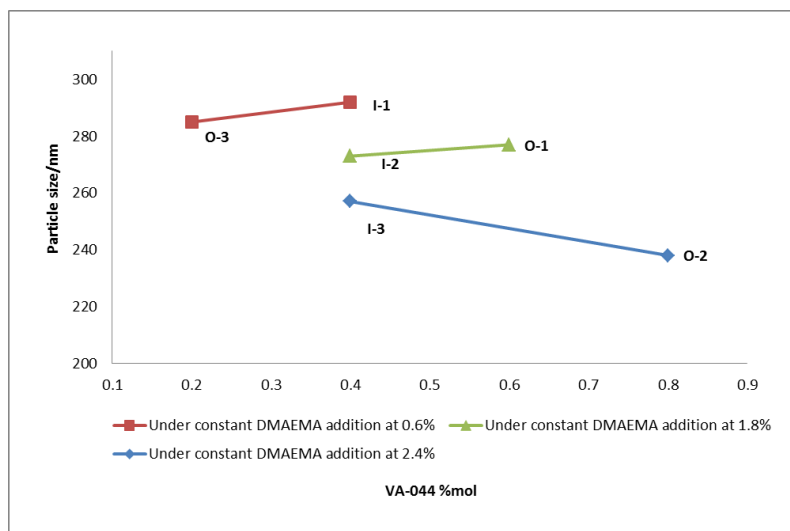


Figure 3.6 Particle size versus concentration of VA-044% at constant DMAEMA levels (0.6%, 1.8% and 2.4%, respectively)

Examining the combined results from series I and series O, the effect of increasing initiator at constant DMAEMA concentration could also be determined (Figure 3.6). Increasing VA-044 concentration at relatively lower DMAEMA levels (0.6% and 1.8%) slightly increased the final particle size indicating that in this range the influence of ionic strength surpassed that of the total stabilizing force. When the DMAEMA loading was higher (2.4%), increasing the initiator amount started to decrease the particle size, in agreement with the particle size trends in series I and series

O. The particle size tuning capacity of VA-044 was limited compared to that of DMAEMA as the range that the concentration of an initiator can be varied is rather restricted. Molar percentage of initiator is usually under 1mol% in order to achieve a reasonable molecular weight and extra addition of initiator is less favourable from an application perspective.

3.3.1.3 Effects of varying solids content (initial monomer concentration)

In the M-series of experiments, the amount of VA-044 and DMAEMA were both kept constant, while the initial MMA monomer loading was varied from 3 ml to 12 ml with an increment of 3 ml at each entry, corresponding to ~5% to ~20% total solids content (Table 3.6). Particle sizes ranged from 212 nm at 5% solids content to 509 nm at 20% solids content. Increasing the monomer concentration led to a decrease in number of particles. The amount of VA-044 available to initiate new polymer chains was the same, as well as the total stabilizing group concentration. However the monomer droplets also require stabilization, which slightly decreases the amount of stabilizing groups initially available for particle stabilization. Overall a lower ratio of stabilizing groups to monomer results in less stabilizing capacity per unit monomer, and hence larger particle size. The polydispersity of the resulting latex was broader in higher solids experiments, behaviour commonly seen in emulsion polymerization.

Table 3.6 SFEP recipe and latex properties with different solid content at 65 °C

| EXP | MMA /ml | H ₂ O /ml | VA-044 /mol% ^a | DMAEMA /mol% ^a | Size /nm | PDI | Zeta | Conv. /% | N _p /(10 ¹⁶ /L) |
|-----|------------|-------------------------|------------------------------|------------------------------|-------------|-------|-------|-------------|--|
| M-1 | 3 | 50 | 0.4 | 1.2 | 212 | 0.024 | +48.6 | 100 | 1.01 |
| N-2 | 6 | 50 | 0.4 | 1.2 | 249 | 0.021 | +54.1 | 95 | 1.16 |
| M-2 | 9 | 50 | 0.4 | 1.2 | 407 | 0.099 | +55.5 | 100 | 0.42 |
| M-3 | 12 | 50 | 0.4 | 1.2 | 509 | 0.161 | +50.1 | 100 | 0.28 |

3.3.1.4 Effects of varying reaction temperatures at different solids content

It has been commonly accepted that the aqueous initiation rate is crucial to particle nucleation in surfactant-free emulsion polymerization.^{21,22} A shorter period of nucleation induced by a higher concentration of radicals produces more uniform particles.²² When the nature and concentration of the initiator were kept constant, the rate of initiation is dominated by temperature. An Arrhenius equation describes the temperature dependence of initiator decomposition (Equation 3.9). A theoretical modeling of the radical generation at different temperatures is shown in Figure 3.7 and calculated using Equation 3.10, under the assumption that VA-044 decomposition was an ideal first order reaction.

$$k_d = A \exp(-E_d/RT) \quad (3.9)$$

$$1 - [I]_t/[I]_0 = 1 - \exp(-k_d t) \quad (3.10)$$

Where, k_d is the initiation decomposition rate constant, $[I]_0$ and $[I]_t$ are the concentrations of initiator at time zero and any reaction time (t) during decomposition, R is the ideal gas constant. $A = 1.22 \times 10^3 / s^{-1}$, is the pre-exponential factor, and $E_d = 1.08 \times 10^5$ J/mol is the activation energy,¹⁷ respectively.

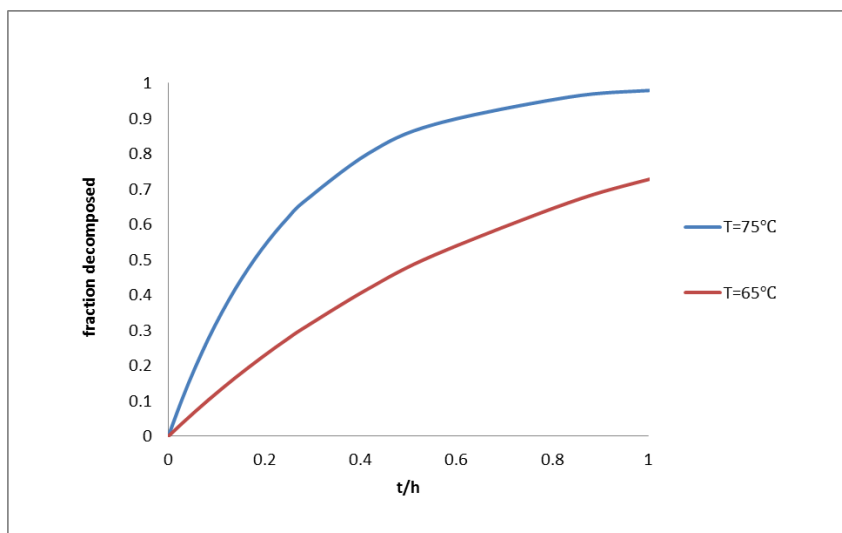


Figure 3.7 Theoretical modeling of temperature dependence of VA-044 decomposition

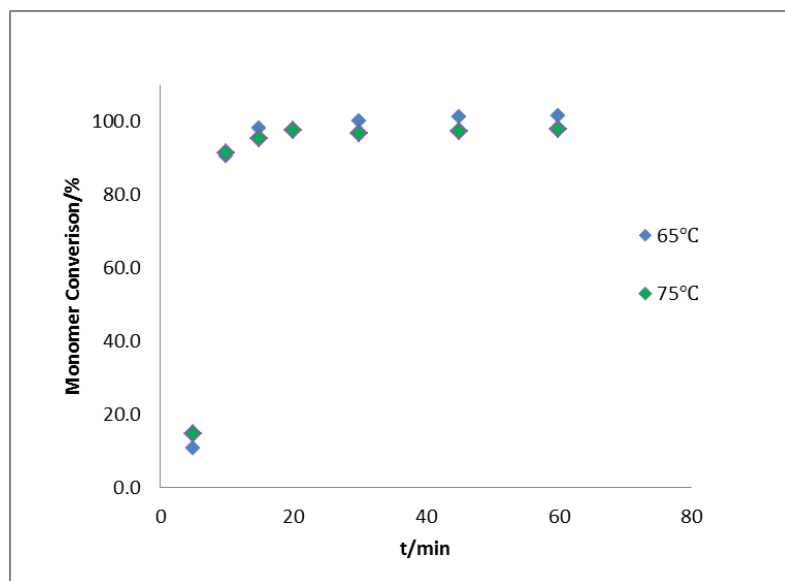


Figure 3.8 Monomer conversion of Entry S-2/N-2 vs. reaction time

Experiment series S was conducted at 75°C in comparison with series M at 65°C. Monomer conversion was monitored throughout the reaction as shown in Figure 3.8. The kinetics at 65°C are almost as fast as at 75°C despite the slower initiation rate of VA-044 shown in Figure 3.7. A

slightly faster nucleation was observed in the entry at 75 °C. A comparatively narrower PDI supports the statement that faster nucleation leads to more uniform particles. This effect was especially outstanding at higher solids content at 20% where the lower temperature entry (M-3) started to have a PDI>0.1 while that of S-4 at higher temperature remained at 0.076. Generally, the PDI in the S series increased when the initial monomer concentration was higher which agreed with the trend observed in the M series.

Table 3.7 SFEP recipe and latex properties with different solids content at 75 °C(S)/65°C(M)

| EXP | MMA /ml | H ₂ O /ml | VA-044 /mol% ^a | DMAEMA /mol% ^a | Size /nm | PDI | Zeta | Conv. /% | N _p /(10 ¹⁶ /L) |
|-----|------------|-------------------------|------------------------------|------------------------------|-------------|-------|-------|-------------|--|
| S-1 | 3 | 50 | 0.4 | 1.2 | 172 | 0.011 | +46.5 | 97 | 1.83 |
| S-2 | 6 | 50 | 0.4 | 1.2 | 234 | 0.036 | +52.2 | 97 | 1.42 |
| S-3 | 9 | 50 | 0.4 | 1.2 | 268 | 0.066 | +50.6 | 100 | 1.43 |
| S-4 | 12 | 50 | 0.4 | 1.2 | 311 | 0.076 | +52.4 | 99 | 1.22 |
| M-1 | 3 | 50 | 0.4 | 1.2 | 212 | 0.024 | +48.6 | 100 | 1.01 |
| N-2 | 6 | 50 | 0.4 | 1.2 | 249 | 0.021 | +54.1 | 95 | 1.16 |
| M-2 | 9 | 50 | 0.4 | 1.2 | 407 | 0.099 | +55.5 | 100 | 0.42 |
| M-3 | 12 | 50 | 0.4 | 1.2 | 509 | 0.161 | +50.1 | 100 | 0.28 |

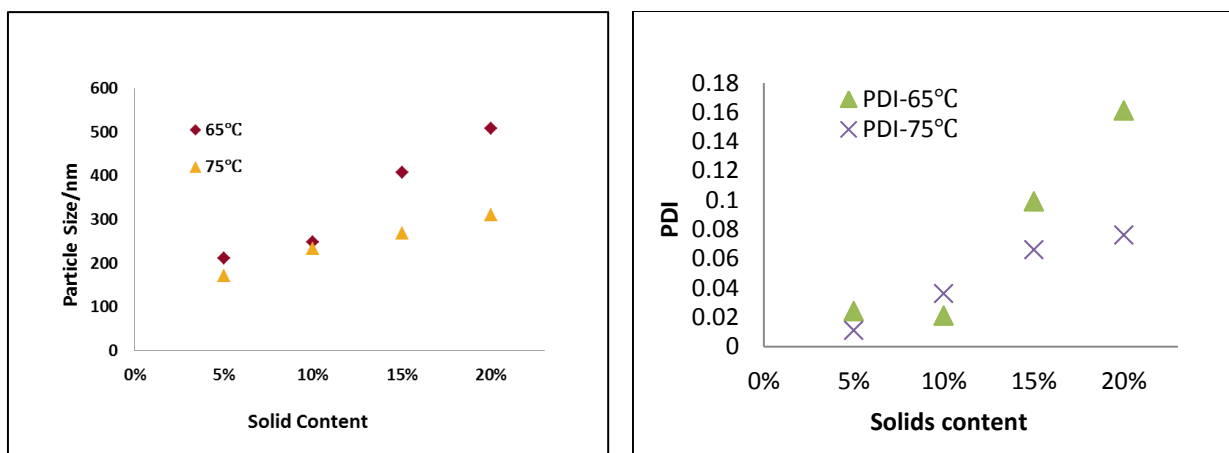


Figure 3.9 Particle size (left) and PDI (right) variation with solids content at 65°C and 75°C

The particle size in each entry in the S series was consistently smaller than M series. The difference was not obvious at lower solids content (Figure 3.9) but became increasingly significant at higher monomer concentration, indicating that higher temperature could be a useful variable to produce smaller particle with high product yield efficiency. The smaller particle size results at higher temperature are likely because of the higher number of particles generated by a higher concentration of radicals. At 75°C, the number and size of particles did not vary as much as that of 65°C. The Charleux²³ group reported a similar phenomenon in the SFEP batch system of methyl methacrylate. They found that when the concentration of the macroinitiator reached 6×10^{-3} mol/L, the monomer concentration no longer had a significant effect on the particle size.

3.3.1.5 Summary of controlling the particle size range

By varying different parameters such as the ratio of initiator and functional comonomer, solids content, amount of total stabilizing groups and reaction temperature, the particle size can be controlled over a wide range as presented in Figure 3.10. Varying initial monomer concentration at 65 °C provided the broadest manipulating potential on the final latex particle size, with a range from 212 nm to 509 nm. The most limited tuning variable was overall number of stabilizing

groups, with a particle size range of 200~300 nm under the investigated experimental conditions. Increasing the temperature to 75°C at the same solids content reduced the gap between the upper and lower limit of particle size because of faster nucleation at higher temperature.

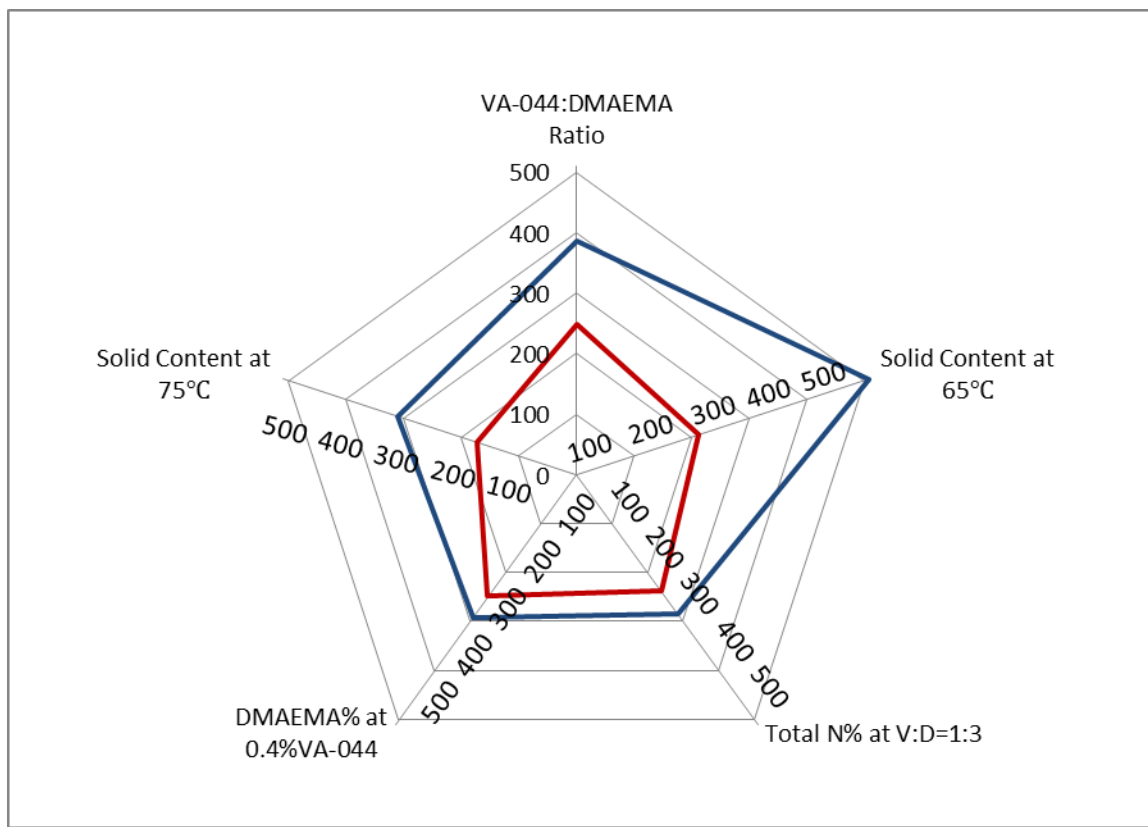
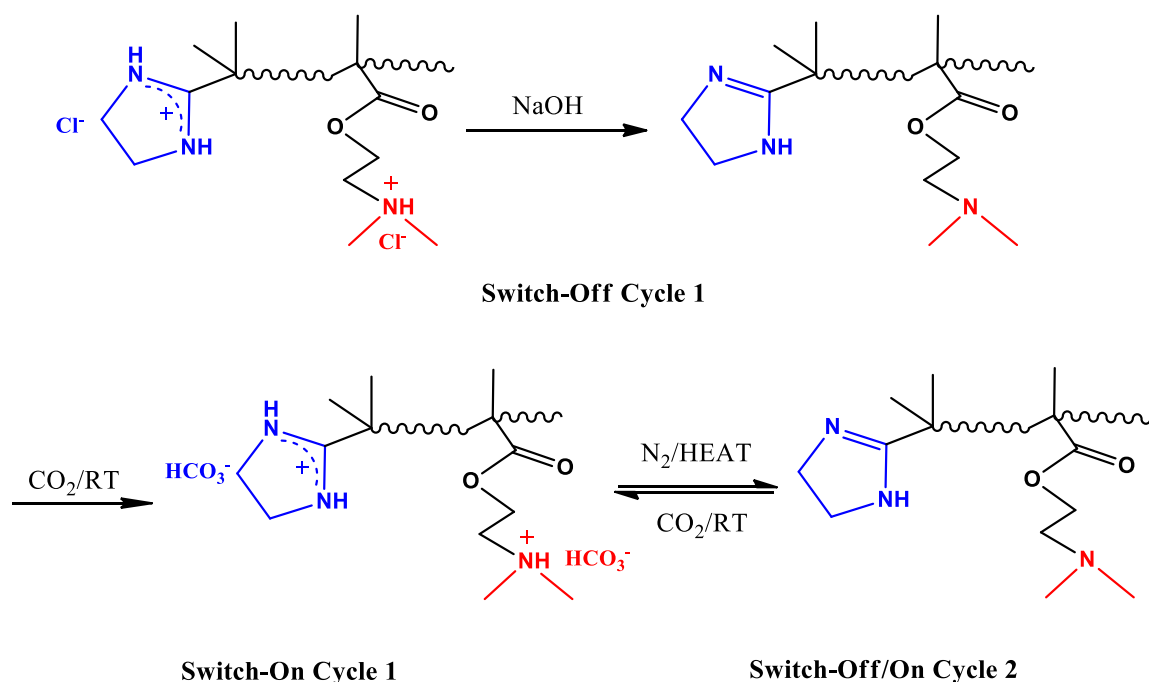


Figure 3.10 Summary of upper/lower range of particle size by varying parameters (nm)

3.3.2 CO₂-switchable performance of PMMA latexes prepared from SFEP

Two switching cycles were successively performed to the latexes obtained in experiment Series N. The first switching-off procedure was triggered by NaOH to neutralize the HCl and in the second cycle by N₂ in a 60°C water bath. Both switching-on cycles were carried out by 5min CO₂ purging. The molecular structure change in each protonation/deprotonation cycle is shown in Scheme 3.2. The first coagulation was previously tried by adding 1.5 times excess NaOH (1M)

followed by 3~4 times washing with distilled water until the pH of the supernatant stopped changing. We reasoned that the same coagulation behaviour could be achieved by carefully adding NaOH dropwise until the pH reached between 9.5~10. The amount of NaOH added to reach the targeted pH turned out to be very close to the equivalent amount of the total N% but always slightly less (within 10%). The reason behind this was probably that a small portion of the N was buried inside the latex particles and could not be neutralized by the NaOH due to diffusion difficulties. The second cycle of switching-off procedure needed heat because the lower critical solution temperature (LCST) of poly(DMAEMA) was around 40 °C⁶ and therefore it would remain water soluble at room temperature even after being deprotonated. Attempts to switch off without heating were therefore not successful. In comparison, switching-off Cycle 1 was successful even under room temperature. This was attributed to the NaCl presence resulting from the neutralization. The concentration of electrolyte to sufficiently coagulate an electrostatic stabilized system is 0.01M.²⁴ The N series had a concentration of overall charged groups at 2% with respect to MMA. After being fully neutralized, it would give a concentration of NaCl at 0.0224 M. The high salt concentration might be playing the major role of destabilizing the emulsion system even at room temperature in Cycle 1 due to the increased ionic strength. However, since after centrifugation in switching-off Cycle 1, the majority of the salt was removed, it would not further affect the second switching-off cycle.

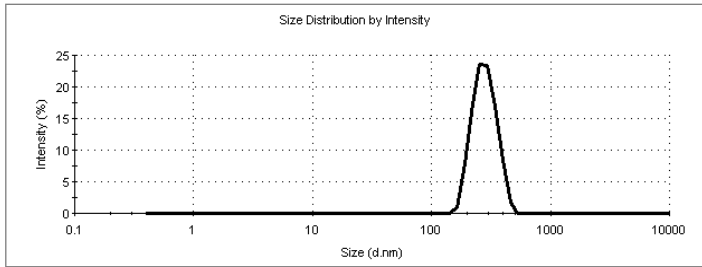


Scheme 3.2 Switching-Off/On cycles in molecular perspective

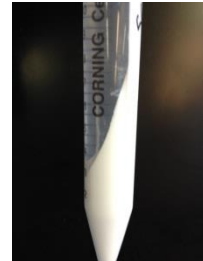
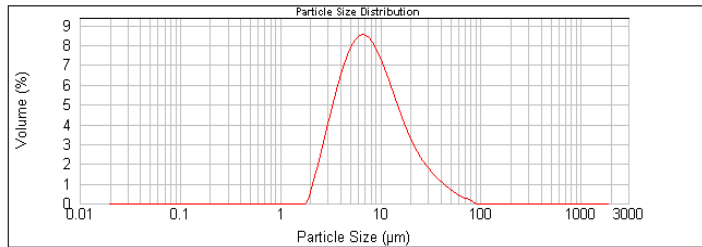
Table 3.8 shows the CO₂ switchable behavior of experimental entries N-1 to N-10. A very fast response to both switching-on and switching-off procedures was observed. In the first cycle the particle size in most entries was almost identical to the original one after 5min CO₂ treatment without further assistance from mechanical stirring. Deviation ($\pm 15\text{nm}$, $\sim 5\%$) was considered within instrumental error. This is a significant improvement compared to literature reports^{11,14} where external energy input such as several minutes of sonication is usually required to recover the particle size and PDI. Monomodal distribution of the colloidal particles after cycle 1 was preserved as indicated by the recovered polydispersity index (< 0.1). Zeta-potential was always slightly lower than the original. This was mainly attributed to the weaker acidity of carbonic acid compared to HCl and the subsequently less efficient protonation by CO₂. After conducting the second switching-off cycle, zeta-potential in almost all entries remained around +30mV, significantly higher than that of the first cycle.

Table 3.8 Latex properties of CO₂-switchable cycles (N-Series)

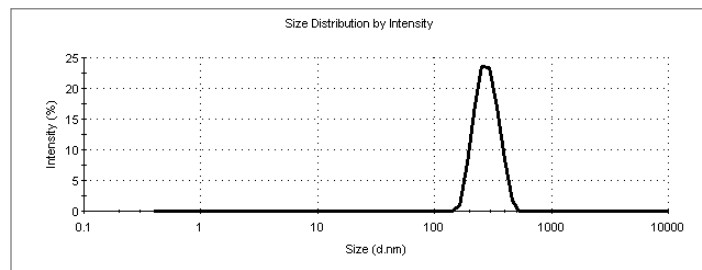
| EXP Parameter | | Original Latex | | | Switching-off 1 NaOH | | Switching-on 1 CO ₂ /5min/RT | | | Switching-off 2 N ₂ /60°C | | Switching-on 2 CO ₂ /5min/RT | | |
|---------------|---|----------------|-------|-------------|-------------------------|-------------|--|-------|-------------|---|-------------|--|-------|-------------|
| Entry | N% _{VA-044} :N% _{DMAEMA} | Size /nm | PDI | Zeta /mV | Size /μm | Zeta /mV | Size /nm | PDI | Zeta /mV | Size /μm | Zeta /mV | Size /nm | PDI | Zeta /mV |
| N-1 | 1:9 | 335 | 0.073 | +64.4 | 6.7 | +18.2 | 328 | 0.072 | +52.9 | 27.0 | +31.9 | 381 | 0.161 | +51.5 |
| N-5 | 1:4 | 283 | 0.020 | +58.2 | 7.6 | +15.5 | 281 | 0.013 | +54.7 | 27.6 | +32.2 | 299 | 0.037 | +50.2 |
| N-6 | 1:2.3 | 268 | 0.016 | +54.9 | 5.3 | +12.6 | 259 | 0.034 | +51.5 | 19.0 | +34.3 | 301 | 0.039 | +50.2 |
| N-2 | 1:1.5 | 249 | 0.021 | +54.1 | 6.4 | +17.1 | 248 | 0.048 | +50.9 | 14.6 | +42.6 | 274 | 0.027 | +51.4 |
| N-7 | 1:1 | 267 | 0.035 | +55.3 | 5.7 | +21.3 | 269 | 0.015 | +53.6 | 12.2 | +24.2 | 332 | 0.084 | +50.1 |
| N-8 | 1:0.67 | 288 | 0.046 | +54.3 | 5.7 | +20.7 | 299 | 0.032 | +54.3 | 13.5 | +24.2 | 445 | 0.146 | +49.5 |
| N-3 | 1:0.43 | 289 | 0.097 | +52.2 | 6.2 | +20.1 | 306 | 0.132 | +50.2 | 10.1 | +29.8 | 495 | 0.195 | +47.4 |
| N-9 | 1:0.25 | 319 | 0.069 | +58.3 | 5.5 | +23.2 | 577 | 0.218 | +51.3 | - | - | - | - | - |
| N-10 | 1:0.11 | 321 | 0.095 | +52.9 | 6.6 | +16.7 | 2866 | 0.415 | +35.8 | - | - | - | - | - |
| N-4 | 1:0 | 387 | 0.136 | +50.2 | 6.2 | +21.0 | 4244 | 0.253 | +26.4 | - | - | - | - | - |



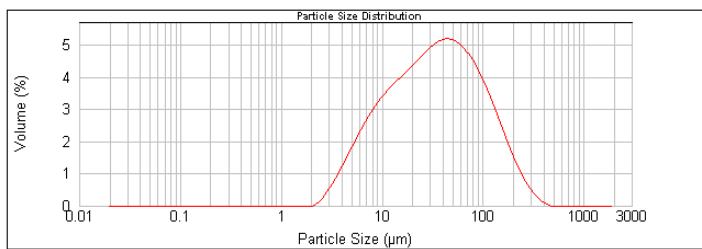
N-5 Original Latex: Size=283nm, PDI=0.02, δ =+58.2mV



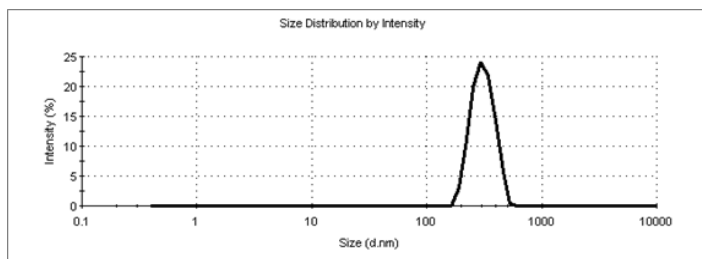
Switching-off Cycle 1 by NaOH: Size=7.6 μ m, δ =+15.5mV



Switching-on Cycle 1 by CO₂/5min/RT: Size=281nm, PDI=0.013, δ =+54.7mV



Switching-off Cycle 2 by N₂/2min/60°C: Size=27.6 μ m, δ =+32.2mV



Switching-on Cycle 2 by CO₂/5min/RT: Size=299nm, PDI=0.037, δ =+50.2mV

Figure 3.11 DLS results and photographs of two switching-off/on cycles of Entry N-5

This was mainly because that the pK_{aH} of the amidine group of VA-044 residual, approximated to 2-ethylimidazoline at 11.05,²⁵ made it easy to be switched on but difficult to be switched off. It was not completely switched off at the given condition bubbling N_2 at $60^\circ C$. However, DLS measurement (Figure 3.11) shows that all the particles had aggregated into large clusters with particle size ~ 10 micrometers without a trace of a particle population at the submicron size range, which was even larger than that in the first switching-off cycle. After the second round of switching-on, particle size for all entries marginally increased compared to Cycle 1, accompanied by a slightly broader polydispersity, while zeta- potential was almost perfectly recovered. The larger aggregates resulting from the second switching-off cycle may have made it more difficult for CO_2 to reach the N atoms inside the clusters and switching-on therefore became less efficient. Significant correlation of the CO_2 response to the ratio of VA-044 and DMAEMA (V:D) was observed. In Cycle 1, as the proportion of VA-044 increased to 80% (N-9, V:D=1:0.5) of the total N%, the system failed to respond to attempts at switching on, and the inertness persisted as the V:D ratio increased. In the absence of DMAEMA, the latex showed almost no response to the CO_2 trigger with latex properties remaining at the similar level as that of the switched off condition. In Cycle 2, N-3 and N-8 demonstrated the most inferior CO_2 -switchable performance with the highest V:D ratio among the entries during this cycle. N-1, with the lowest V:D ratio at 1:18, also experienced only partial recovery of the particle size distribution with an increased PDI to 0.161. The CO_2 response was closely related to the particle size. Entry N-2 obtained the smallest size and the best CO_2 switchable performance.

3.3.2.1 Boundary conditions for achieving CO_2 -switchable behavior

With numerous experiments completed, we were in a position to identify the approximate boundaries of where we could still achieve reasonable switchability but with a minimum number of switchable groups required. The number of stabilizing groups could be reduced by half with only 36 nm growth in particle size, as seen by comparing Entries O-3 (285 nm, 1% total N%) and

N-2 (249 nm, 2% total N%). Meanwhile, a 10-degree increase in temperature could significantly reduce particle size from 509 nm (S-4, 75 °C) to 311 nm (M-4, 65°C) with moderately high solids content at 20%. The lowest overall N⁺% at 1mol/L (O-3) and the highest solids content at 20% (S-4) were the two boundary conditions in our system. Therefore, two switching-on/off cycles were performed with O-3 and S-4 to test the CO₂-responsive performance.

Table 3.9 Latex properties during switching cycles (O-3 & S-4)

| Entry | O-3 | | | S-4 | | |
|-----------------------|---------|-------|----------|---------|-------|----------|
| | Size | PDI | Zeta /mV | Size | PDI | Zeta /mV |
| Original | 285 nm | 0.020 | +57.5 | 311 nm | 0.076 | +52.4 |
| Switching-off Cycle 1 | 5.5 μm | - | +14.3 | 3.8 μm | - | +11.4 |
| Switching-on Cycle 1 | 306 nm | 0.069 | +51.9 | 329 nm | 0.082 | +48.9 |
| Switching-off Cycle 2 | 10.7 μm | - | +22.3 | 17.2 μm | - | +35.5 |
| Switching-on Cycle 2 | 445 nm | 0.169 | +51.1 | 399 nm | 0.036 | +49.3 |

For Entry O-3 with 1% total N⁺ groups, particle size grew larger with a broader PDI after each cycle. Especially after Cycle 2, PDI exceeded 0.1 and particle size climbed above 400 nm. Reducing the surface active agent decreased the sensitivity towards CO₂ of the resulting latex. Increasing the solids content to 20% at 75°C yielded better CO₂-switchability, with well preserved PDI and only slightly larger particle size. It is possible that there are more optimizing opportunities beyond the investigated conditions to reduce the overall amount of stabilizing species as well as to increase solid content while obtaining a reasonable CO₂ response.

3.4 Conclusion

Surfactant-free emulsion polymerization was carried out to produce a series of poly(methyl methacrylate) latexes with demonstrated CO₂-switchable properties. The responses to triggers in

either switching-on or switching-off procedures were both effective and fast. The most significant breakthrough in the current work compared to previous studies was that the redispersion process was free from the need for intense mixing or sonication. The two switching-on procedures both only required 5min bubbling CO₂ into the system without further energy input. The first switching-off cycle could be achieved by NaOH addition without further need of washing, while the second cycle of switching-off (N₂ bubbling for less than 5min) needed mild heating. The particle size of the latex was fine-tuned over a range from 170 ~500 nm by varying parameters such as the ratio of initiator VA-044 and functional comonomer DMAEMA. Most experimental entries exhibited narrow PSD with a PDI<0.1. A positive correlation between the particle size and the CO₂-switchable performance were also observed, with the smallest particle size yielding the best CO₂-response. The overall loading of added stabilizing groups could be reduced to as low as 1% N⁺(VA-044+DMAEMA) while maintaining good latex properties (particle size=285 nm, PDI=0.020, zeta-potential=+57.5 mV).

References

- (1) Van de Wetering, P.; Moret, E. E.; Schuurmans-Nieuwenbroek, N. M.; van Steenberg, M. J.; Hennink, W. E. *Bioconjug. Chem.* **1999**, *10*, 589–597.
- (2) Liu, Y.; Jessop, P. G.; Cunningham, M.; Eckert, C. a; Liotta, C. L. *Science* **2006**, *313*, 958–960.
- (3) Tan, B. H.; Ravi, P.; Tam, K. C. *Macromol. Rapid Commun.* **2006**, *27*, 522–528.
- (4) Yan, B.; Han, D.; Boissière, O.; Ayotte, P.; Zhao, Y. *Soft Matter* **2013**, *9*, 2011–2016.
- (5) Kumar, S.; Tong, X.; Dory, Y. L.; Lepage, M.; Zhao, Y. *Chem. Commun. (Camb)*. **2013**, *49*, 90–92.
- (6) Han, D.; Tong, X.; Boissière, O.; Zhao, Y. *ACS Macro Lett.* **2012**, *1*, 57–61.
- (7) Zhang, Q.; Yu, G.; Wang, W.-J.; Li, B.-G.; Zhu, S. *Macromol. Rapid Commun.* **2012**, *33*, 916–921.
- (8) Zhang, Q.; Yu, G.; Wang, W.-J.; Yuan, H.; Li, B.-G.; Zhu, S. *Macromolecules* **2013**, *46*, 1261–1267.
- (9) Pinaud, J.; Kowal, E.; Cunningham, M.; Jessop, P. *ACS Macro Lett.* **2012**, *1*, 1103–1107.
- (10) Zhang, Q.; Wang, W.-J.; Lu, Y.; Li, B.-G.; Zhu, S. *Macromolecules* **2011**, *44*, 6539–6545.
- (11) Zhu, S. *Macromol. Rapid Commun.* **2012**, *33*, 916–921.
- (12) Zhang, Q.; Yu, G.; Wang, W.-J.; Yuan, H.; Li, B.-G.; Zhu, S. *Macromolecules* **2013**, *46*, 1261–1267.
- (13) Su, X.; Jessop, P. G.; Cunningham, M. F. *Macromolecules* **2012**, *45*, 666–670.
- (14) Pinaud, J.; Kowal, E.; Cunningham, M.; Jessop, P. *ACS Macro Lett.* **2012**, *1*, 1103–1107.
- (15) BASF. *N, N-Dimethylaminoethyl Methacrylate (DMAEMA)* **2011**, 1–3.
- (16) Mitsubishi Gas Chemical Company, I. *SIDS Initial Assess. Rep. 2-Dimethylaminoethylmethacrylate* **2002**.
- (17) Wako Pure Chemical Industries Ltd. <http://www.wako-chem.co.jp/specialty/waterazo/VA-044.htm>.
- (18) Hearn, J.; Ottewill, R. H.; Shaw, J. N. *Br. Polym. J.* **1970**, *2*, 116–120.

- (19) Van den Hul, H. J.; Vanderhoff, J. W. *Br. Polym. J.* **1970**, *2*, 121–127.
- (20) Ngai, T.; Wu, C. *Langmuir* **2005**, *21*, 8520–8525.
- (21) Kuehn, I.; Tauer, K. *Macromolecules* **1995**, *28*, 8122–8128.
- (22) Bao, J.; Zhang, A. *J. Appl. Polym. Sci.* **2004**, *93*, 2815–2820.
- (23) Dire, C.; Magnet, S.; Couvreur, L.; Charleux, B. *Macromolecules* **2009**, *42*, 95–103.
- (24) Romero-Cano, M. S.; Martín-Rodríguez, A.; de las Nieves, F. J. *Langmuir* **2001**, *17*, 3505–3511.
- (25) Elguero, J.; Gonzales, E.; Imbach, J.L.; Jacquier, R. *Bull. la Société Chim. Fr.* **1968**, *11*, 4075–4077.

Chapter 4

A comprehensive characteristic study of functional comonomer DEAEMA/DMAEMA used in surfactant-free emulsion polymerization

Abstract Detailed characterization of N,N-diethylaminoethyl Methacrylate (DEAEMA) and N,N-dimethylaminoethyl Methacrylate (DMAEMA) was carried out on hydrolysis degree and protonation efficiency using ^1H NMR. An astonishingly high hydrolysis degree of 71% for DEAEMA and 84% for DMAEMA at 65 °C within 4 hours was observed in a CO_2 saturated aqueous phase. The high hydrolysis degree was believed to be the major cause of their inferior performance as functional comonomers under CO_2 protonation compared to HCl protonation in the surfactant-free emulsion polymerization of methyl methacrylate. The reversible protonation of CO_2 was proposed to be the cause of significant hydrolysis even at a high degree of protonation. A relatively hydrolysis-free operational window in terms of pH and temperature choices was defined under HCl and CO_2 protonation, respectively.

4.1 Introduction

During the exploration of CO₂-switchable nanoparticle systems, DMAEMA and DEAEMA have been popularly employed as responsive agents¹⁻³. It is important for researchers to acquire some basic understanding of the monomer behaviors when they are utilized in CO₂ switchable systems. The acidic aqueous environment resulted from CO₂ saturation will bring in enhanced hydrophobicity, protonation of the monomer molecules as well as the inevitable challenge of ester hydrolysis. This work seeks to provide some supplementary information towards a comprehensive understanding of the functional comonomers as well as insight and direction for further experimental development.

4.2 Experimental Section

4.2.1 Materials

Chemical compounds N,N-Diethylaminoethyl Methacrylate (DEAEMA, Aldrich, 99%), hydrochloric acid (HCl, Aldrich), deuterated water (D₂O, Cambridge Isotope Laborites) 2,2'-azobis[2-(2-imidazolin-2-yl)propane] (VA-061, Wako), 2,2'-azobis[2-(2-imidazolin-2-yl)propane]dihydrochloride (VA-044, Wako), carbon dioxide (CO₂, Praxair, Medical Degree) and nitrogen (N₂, Praxair, Ultra High Purity, 5.0) were used as received. Inhibitor removal columns were used to purify monomers. Distilled and deionized water used for all experiments was purified through a Synergy ion exchange unit supplied by Millipore.

4.2.2 Determination of protonation efficiency and hydrolysis degree by ¹H NMR

In a typical experiment, 20 μl of DEAEMA/DMAEMA was added into an NMR tube with a mixture of 60 μl deuterated water and 540 μl distilled water (90% H₂O+10% D₂O). CO₂ was purged into the NMR tube equipped with a rubber cap using a 20-gauge needle for 5 min at room temperature to promote dissolution, followed by another 5 min at the investigated temperature.

The NMR tube was sealed by paraffin film before being placed into pre-heated NMR facility at the test temperature and a ^1H NMR spectra was immediately acquired.

Experiments with 0, 0.25, 0.50, 0.75, 1.0 and 1.5 equivalents of HCl with respect to 20 μl of DMAEMA were also performed to determine the standard curve of protonation efficiency of DMAEMA. 25°C (R.T.), 45°C and 65°C were chosen to examine the temperature dependence of protonation efficiency at CO_2 -saturation.

A hydrolysis study was also carried out by ^1H NMR. 1 ml of inhibited DEAEMA/DMAEMA was added into 30 ml of distilled water, and purged by CO_2 for 10 min in an ice bath. A sample was taken as soon as the reactor was immersed into the pre-heated oil bath and 0.1 ml of sample was transferred into 0.4 ml of deuterated water (D_2O) and instantly put into a mixture of ice and water prior to NMR acquisition. In certain entries, the pH of the reaction system was adjusted by adding 1.25 M HCl dropwise under instant pH meter readings. A sample was withdrawn every hour for a total of 4 hours.

4.2.3 Surfactant-free emulsion polymerization using VA-061/VA-044 and DEAEMA

Emulsion polymerization was carried out on a six-well carousel reactor (Radley's Innovation Technology) with one flask bearing a thermometer immersed in the same amount of water as the reaction vessels as a reference of real reaction temperature. Three reactions were run parallel each time. 50 ml distilled water was first heated up to 65 °C in a flask with constant CO_2 bubbling, while VA-061 and DEAEMA were added into separate 20 ml scintillation vials with 5 ml water, respectively, and purged with CO_2 in an ice bath to complete dissolution. DEAEMA was first charged into the heated water, prior to injection of CO_2 pre-purged MMA and then initiator solution was added to start the reaction. The flasks were sealed without gas bubbling during the reaction. A minor difference in an experiment carried out with HCl was that DEAEMA was added into 55 ml water directly and the pH of the solution was first adjusted to ~4 by HCl

(1.25M) prior to increasing to the reaction temperature, and the purging gas used was N₂. All experiments were set under an agitating speed of 8 and run for 2 hours. A sample was withdrawn at the end of reaction for DLS analyses as well as conversion determination.

4.3 Characterization

Monomer conversions were determined gravimetrically. 2-4 ml samples were withdrawn and cooled immediately in an ice bath to stop further polymerization. Samples were first dried under air flow overnight at room temperature and in a vacuum oven for another 12 hours. Conversion was calculated as follows:

$$\text{conversion} = \frac{(M_{\text{dry}})(M_{\text{MMA}} + M_{\text{DEAEMA}} + M_{\text{I}} + M_{\text{water}})}{M_{\text{wet}}(M_{\text{MMA}} + M_{\text{DEAEMA}} + M_{\text{I}})} \quad (4.1)$$

Where M_{MMA} , M_{DEAEMA} , M_{I} , M_{water} are the mass of MMA, DEAEMA, initiator and water, respectively; and M_{dry} , M_{wet} are the mass of the latex sample and the mass of the dried polymer. Particle size and zeta-potential were measured on a Malvern Zetasizer Nano ZS (size range 0.6 nm to 6 μm) at 25°C using a disposable capillary cuvette and a universal dip cell (DTS1070). Samples were diluted with distilled water for experiments carried out with HCl protonation and CO₂ saturated water for those with CO₂ protonation prior to measurement. The refractive index of the copolymer was approximated by that of PMMA. A Thermo Scientific Orion Star A215 calibrated with aqueous standards (pH 4, 7, and 10) was used to adjust pH. A Bruker Avance-400 (DRX) was used for determination of the hydrolysis degree while a Bruker Avance-500 (DRX) equipped with an FTS air system for temperature control was utilized for the protonation efficiency study.

Protonation efficiency was calculated based on the following equation:⁴

$$\text{Protonation Efficiency from Proton X} = \frac{\delta_x - \delta_{0\%}}{\delta_{100\%} - \delta_{0\%}} \quad (4.2)$$

Where δ_x , $\delta_{0\%}$ and $\delta_{100\%}$ are the chemical shifts of Proton X at a certain protonation condition, 0% protonation and 100% protonation, respectively. The final protonation efficiency was calculated as an average of the two proton species A and B.

4.4 Results and discussion

4.4.1 Surfactant-free emulsion polymerization using VA-044/VA061 and DEAEMA

In an early attempt to conduct surfactant-free emulsion polymerization under a CO₂ saturated environment, a semi-batch seed-feed approach was employed in order to maximize the proportion of the functional comonomer distributed on the particle surface. An emulsion seed was first prepared with all the intended DEAEMA and small fraction of MMA, followed by constant feeding of MMA at a slow speed (1-2.5 ml/h) to carry on the polymerization. Ideally DEAEMA would be all consumed in the seed stage and therefore remain on the particle surface. The properties of the seed were first studied to define an optimized VA-061:DEAEMA ratio for smallest size and highest latex stability (Table 4.1). However, even with a solids content as low as 2.5%, the smallest particle size that could be obtained from this method was ~200 nm, which was not ideal for an emulsion seed. It was also observed that as the DEAEMA:VA-061 ratio increased, the latex properties tended to be inferior with a higher PDI and a lower zeta-potential as well as an increased particle size.

Table 4.1 The seeds properties under different DEAEMA:VA-061 ratio

| Entry | D:M Ratio | Latex Properties | | | | |
|--------|-----------|------------------|------------------------|------|-------|--------|
| | (mol:mol) | Size/nm | Np/10 ¹⁴ /L | PDI | ζ/mV | Conv.% |
| 25-B-1 | 2:1 | 797 | 0.08 | 0.19 | +20 | 82.4 |
| 25-B-2 | 1:1 | 574 | 0.19 | 0.07 | +24.9 | 72.7 |
| 25-B-3 | 1:2 | 374 | 0.79 | 0.11 | +30.4 | 84.8 |
| 25-B-4 | 1:4 | 262 | 2.08 | 0.02 | +35.5 | 76.5 |
| 25-B-5 | 1:8 | 227 | 2.92 | 0.03 | +47.1 | 69.6 |
| 25-B-6 | 1:16 | 177 | 7.73 | 0.04 | +50.2 | 87.5 |
| 25-B-7 | 1:32 | 223 | 4.34 | 0.05 | +51.4 | 98.2 |
| 25-B-8 | 1:192 | 222 | 4.40 | 0.02 | +48.7 | 98.2 |
| 25-B-9 | 0 | 235 | 3.65 | 0.02 | +44.7 | 96.7 |

*Seed conditions: 1%_{wt} VA-061, 2.5% solids content, 65°C.

The role of DEAEMA was to act as the in situ generated surface active agent. The larger amount of surfactant generated, the more stabilization the system would possess, which would be reflected in smaller particle size and a larger number of particles. However, the particle size evolution showed the opposite trend (Table 4.1). To further examine the cause, a comparative series of SFEP experiments were conducted under both CO₂ and hydrochloric acid (HCl) protonation (Table 4.2). Entries 25-B-7 to 25-B-9 demonstrated the highest conversion and relatively small particle size with least addition of DEAEMA. The corresponding recipes were used with increased solids content to ~10% and comparative experiments were carried out with either CO₂ protonation or HCl protonation as shown in Table 4.2.

Table 4.2 Comparison of latex properties under CO₂ and HCl protonation

| EXP | Reaction Condition | DEAEMA mol% | Latex properties | | | |
|-----|------------------------|----------------|-----------------------------|------------|-------|-----------------------------|
| | | | Size/PDI nm | Zeta mV | Conv. | Np (10 ¹⁶ /L) |
| A-1 | VA-044/HCl | 3 (1:32) | 203/0.01 | +57 | 96 | 1.88 |
| A-2 | VA-044/HCl | 0.54 (1:192) | 230/0.01 | +50 | 92 | 1.23 |
| A-3 | VA-044/HCl | 0 | 299/0.02 | +50 | 100 | 0.61 |
| B-1 | VA-061/CO ₂ | 3 | 531nm/55.4% 3857nm/44.6% | +23 | 90 | 0.02 |
| B-2 | VA-061/CO ₂ | 0.54 | 323/0.11 | +50 | 90 | 0.44 |
| B-3 | VA-061/CO ₂ | 0 | 344/0.19 | +38 | 93 | 0.37 |

General recipe: VA-044/VA-061/MMA+DEAEMA/H₂O=0.24mmol/0.24mmol/6g/60ml

VA-044 is the hydrochloride salt of VA-061. Under acidic conditions such as a CO₂-saturated aqueous solution, VA-061 is present as its bicarbonate salt and exhibits very similar decomposition behavior to that of VA-044, with the same activation energy as well as a 10 hours half-life at 42°C compared to that of VA-044 at 44°C.⁵ Three experiments using each initiator were carried out, respectively, with increasing amount of DEAEMA as a functional comonomer in its bicarbonate and hydrochloride salt forms.

Cunningham and coworkers⁶ reported that adding small amounts of DEAEMA (0.54mol%) could lead to a significant 50% increase in the number of particles, and subsequently increase the conversion of monomer in the SFEP of styrene from 64% to 90%, mainly attributed to the enhanced aqueous nucleation at the beginning stage of polymerization assisted by the hydrophilic DEAEMA⁺HCO₃⁻. In the Experiment A series, the relatively hydrophilic nature of MMA compared to styrene could promote aqueous nucleation itself and therefore, the importance of DEAEMA in terms of reducing the inhibition period of reaction and increasing conversion was

diminished. Fast kinetics and nearly full conversion were observed within 1 hour regardless of the amount of DEAEMA added into the system.

In Series A, where polymerization was carried out with HCl protonation, a significant reduction of particle size was obtained by increasing the percentage of DEAEMA and incorporated into the copolymer with a constantly preserved narrow PDI (<0.1) featuring nearly monodispersed latex particles. This trend obeyed the general rule in emulsion polymerization that there should be a negative correlation between the amount of surfactant and the particle size. The major contribution of DEAEMA in terms of polymerization dynamics was that a small amount could significantly increase the number of particles, which in this case, doubled with 0.54% and tripled with 3% addition. The smaller particle size was indeed a reflection of the promoted nucleation contributed by $\text{DEAEMA}^+\text{Cl}^-$ acting as surface active agent together with the residual groups of VA-044. All three entries demonstrated high zeta-potential ($\geq +50\text{mV}$) indicating a superior colloidal stability from SFEP. A slight increase of zeta-potential with the proportion of DEAEMA could be explained in that there was higher concentration of charged species in the system and subsequently enhanced probability of increased surface charge density. The residual groups of the cationic initiator VA-044 alone could provide adequate electrostatic stabilization that produced latex with a zeta-potential at $+50\text{ mV}$.

In Series B, conversions were slightly lower than that of Series A, while the number of particles was significantly less. However, as observed in the B-25 experiment, 3% addition of DEAEMA produced significantly larger particles and therefore fewer particles than for Entry B-3 where there was no DEAEMA addition. DLS showed that a second peak appeared in the size range $1\ \mu\text{m}$ to $10\ \mu\text{m}$ (Figure 4.1), indicating particle coagulation might have taken place. Meanwhile, the zeta-potential of B-1 was lower than B-2. B-1 was expected to have a higher zeta-potential with a higher charge density. This observation suggested that other factors contributed to the particle stabilization behaviour.

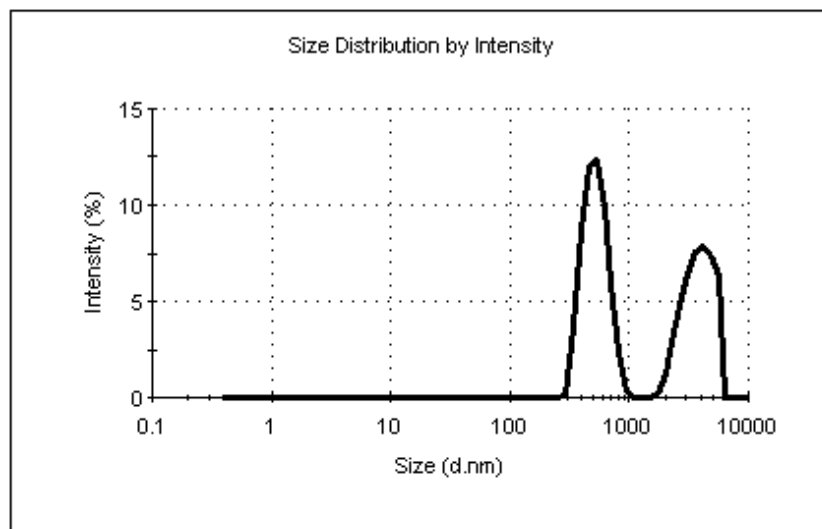


Figure 4.1 Bimodal size distribution of B-1 (531 nm/55.4%; 3857 nm/44.6%)

4.4.2 Determination of protonation efficiency of DMAEMA by ^1H NMR

The first suspected cause of this anomalous behaviour was the lower protonation by carbonic acid compared to HCl. Precise calculation of protonation efficiency of DEAEMA as well as its methyl counterpart was carried out by ^1H NMR. In a mixture of the neutral form as well as the cationic form of DEAEMA/DMAEMA, the protons neighbouring to the nitrogen of the tertiary amine will exchange between the charged/uncharged species at a certain speed. If slower than the NMR acquisition, two individual peaks representing each species can be read in the resulting NMR spectrum; if faster the two peaks will merge into a single peak that can be found at a chemical shift in between those of the original two peaks. In the latter case, the formula below can be used to theoretically calculate the observed chemical shift,

$$\delta_{\text{observed}} = \delta_{\text{neutral}}x_{\text{neutral}} + \delta_{\text{cationic}}x_{\text{cationic}} \quad (4.3)$$

Where δ_{observed} , δ_{neutral} , δ_{cationic} represent the chemical shifts of the merged, the neutral and the cationic read in ^1H NMR spectrum, respectively, and x_{neutral} , x_{cationic} are the mole fractions of each species.

To test the theory, a standard curve by HCl (1 M) protonation at 0, 0.25, 0.50, 0.75, 1.0 as well as 1.5 times equivalents of DMAEMA was generated. Agreement between the theoretical and experimental change in chemical shift was obtained with an R^2 value at 0.999, which confirmed the method was valid. Due to the limited solubility of DEAEMA in the aqueous phase, a standard curve of DEAEMA could not be accurately made as well as an evaluation of the monomer protonation efficiency under a pure water environment. However, as a stronger base than DMAEMA, with a slightly higher pK_{aH} at 8.8 compared to that of DMAEMA at 8.3,⁷ a lower percentage of protonation could be expected.

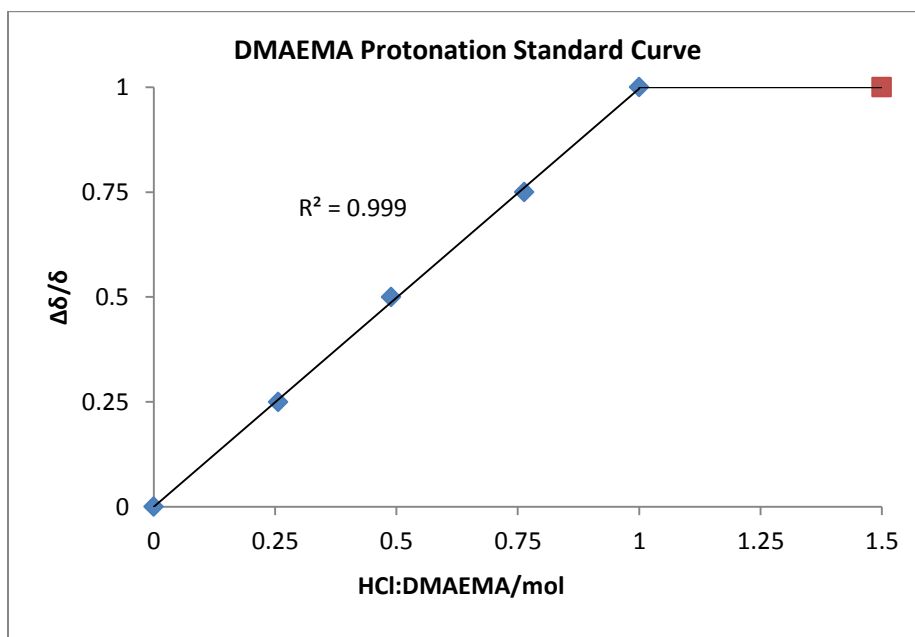


Figure 4.2 Standard curve of HCl protonation of DMAEMA

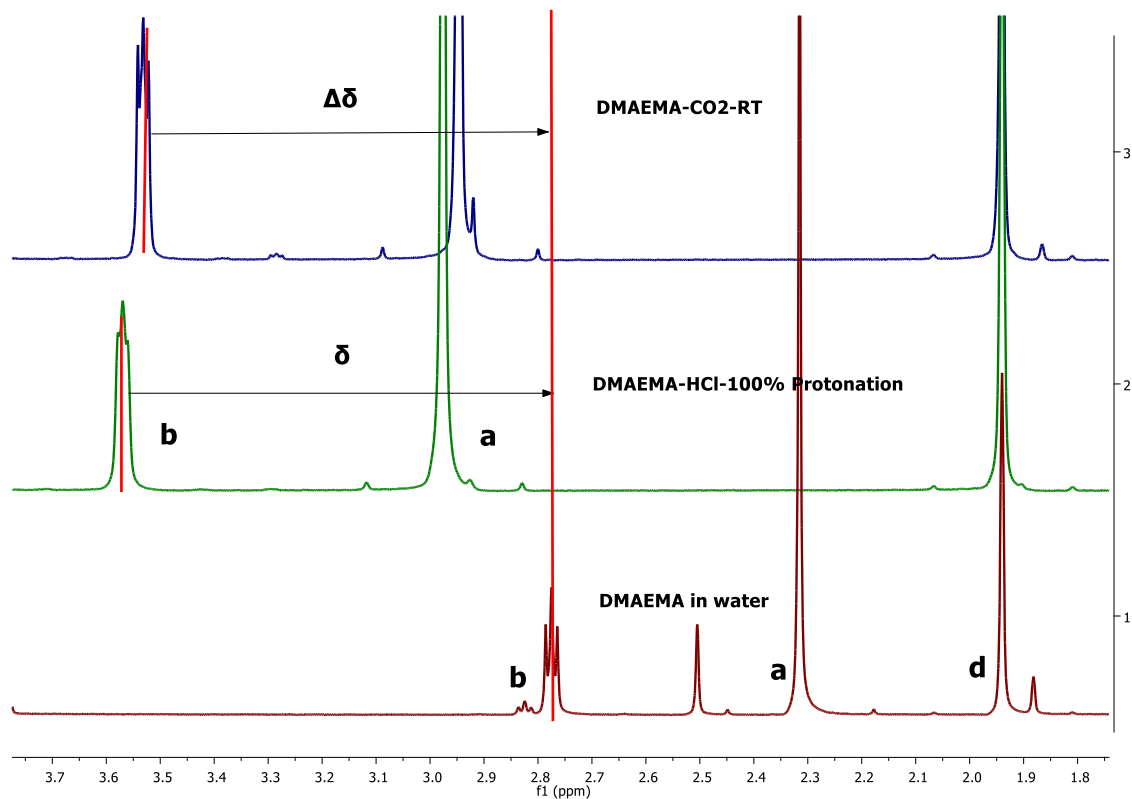
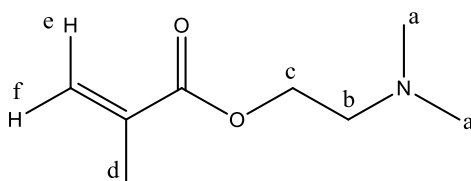


Figure 4.3 Calculation of protonation efficiency of DMAEMA at CO₂ saturated acidity at room temperature (94%)



Scheme 4.1 NMR peak assignment in DMAEMA

Using the verified NMR technique, CO₂ protonation efficiency under different temperatures was examined, and an example of protonation efficiency calculation from NMR spectrum as shown in Figure 4.3. Detailed information on chemical shifts and the calculated protonation efficiencies at higher temperatures was given in Table 4.3. CO₂ has a lower solubility at higher temperatures,

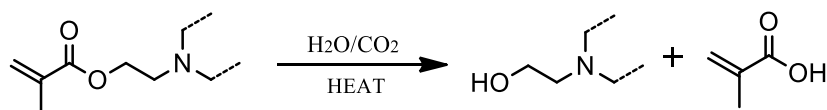
which gives its saturated aqueous solutions a less acidic environment. Protonation is therefore weakened at high temperature due to a lower concentration of reactant. On the other hand, thermodynamically, protonation is an exothermic neutralization reaction and would be promoted by lower temperature. The decrease protonation efficiency of DMAEMA with temperature was not significant, with 94% at room temperature, 90% at 45 °C and 84% at 65 °C. Although the accurate protonation value of that of DEAEMA could not be acquired using this method, it would be a fair assumption that the same insignificance in the temperature dependence of protonation efficiency would apply to DEAEMA as well. The slight difference in protonation efficiency led us to believe there would be other possibilities responsible for the significantly lower efficiency of DEAEMA/DMAEMA as functional comonomers under CO₂ protonation.

Table 4.3 Temperature dependence of protonation of DMAEMA at CO₂ saturated acidity

| Sample | δA (%Protonation) | δB (%Protonation) | Average% Protonation Efficiency |
|----------------------------|------------------------------|------------------------------|------------------------------------|
| | 2.43 | 2.89 | |
| REF-0%-45 °C | (0) | (0) | 0 |
| | 3.11 | 3.70 | |
| REF-100%-45 °C | (100) | (100) | 100 |
| | 3.04 | 3.62 | |
| EXP-CO ₂ -45 °C | (89.7) | (90.1) | 90 |
| | 2.69 | 2.98 | |
| REF-0%-65 °C | (0) | (0) | 0 |
| | 3.25 | 3.84 | |
| REF-100%-65 °C | (100) | (100) | 100 |
| | 3.15 | 3.71 | |
| EXP-CO ₂ -65 °C | (82.1) | (84.9) | 84 |

4.4.3 Determination of monomer hydrolysis of DEMA/DEMAEMA by ¹HNMR

Early literature reports showed that there would be considerable amount of hydrolysis of DMAEMA in a basic aqueous phase⁸. For a CO₂-responsive latex system prepared from surfactant-free emulsion polymerization with DEAEMA/DMAEMA as the functional comonomer, degree of hydrolysis of the ester group (Scheme 4.2) plays a critical role on the performance in terms of determining the colloidal properties. It leads to a direct loss of the functional amine groups. The acid product once absorbed or covalently bonded onto polymer particles, would then produce potential anionic charges on the particle surface interfering with the electrostatic double layer, and subsequently lowering the latex stability.

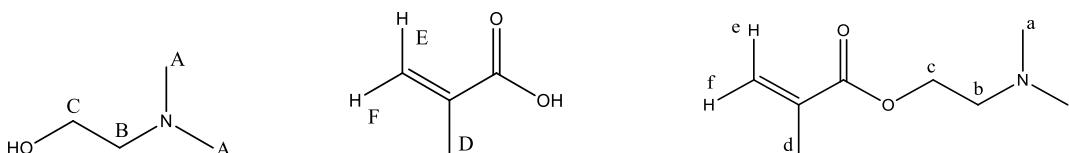


Scheme 4.2 Hydrolysis of DMAEMA/DEAEMA (DEAEMA shown by dashed line)

The statistics reported on the hydrolytic stability of DMAEMA at 37 °C⁸ showed that the hydrolysis rate was slower at a lower temperature (reaction rate constant $k_h=5.2\times 10^{-6} \text{ s}^{-1}$ at pH 7, 37 °C) and the amount of hydrolysis generated during the time interval between taking the sample and performing NMR (<1h, ice bath) was negligible. The same paper also reported the insensitivity of its homopolymer poly(DMAEMA) ($k_h=7\times 10^{-8} \text{ s}^{-1}$ at 80 °C, pH=7) to hydrolysis; therefore, polymer hydrolysis is no longer of interest in this work.

A general NMR summary on hydrolysis is illustrated in Figure 4.4. The most significant chemical shift changes were that of the protons on the double bond and that of the methyl group before and after hydrolysis. Only the ratio of integration of the methyl group was employed to calculate the degree of hydrolysis by $D/(d+D)$ (Scheme 4.3), while these of the protons on the terminal olefin were overlapped slightly by the broad water peak, which would lead to over estimation. Figure

4.4 indicates approximate pseudo first-order reaction kinetics. The rate constants and half-life of hydrolysis are shown in Table 4.3. The calculated half-life at 65 °C was longer than the one displayed in Figure 4.4, mainly due to the relatively low R^2 (0.94) during the plot $\log[A]$ versus t , while that at 45 °C gave a very good prediction at an R^2 value >0.99 (Appendix B). Temperature played a significant role on the hydrolyzing rate, as there was only 2% hydrolysis within four hours at room temperature; while at 65 °C 84% of DMAEMA was hydrolyzed with a half-life less than an hour. Similar temperature dependence was also observed with its ethyl counterpart DEAEMA. While comparing the hydrolyzing behaviors of these two monomers, it was not surprising to find that DEAEMA exhibited a slower rate at all investigated temperatures, which was mainly attributed to a slightly larger steric effect introduced by the two ethyl groups in DEAEMA compared to the methyl groups in DMAEMA. The larger steric hindrance slowed down the interaction of water molecular and the nitrogen atom in DEAEMA. It also created a more hydrophobic environment around the nitrogen atom and shielded the amine group from H_2O molecules.



Scheme 4.3 NMR peak assignment for DMAEMA hydrolysis

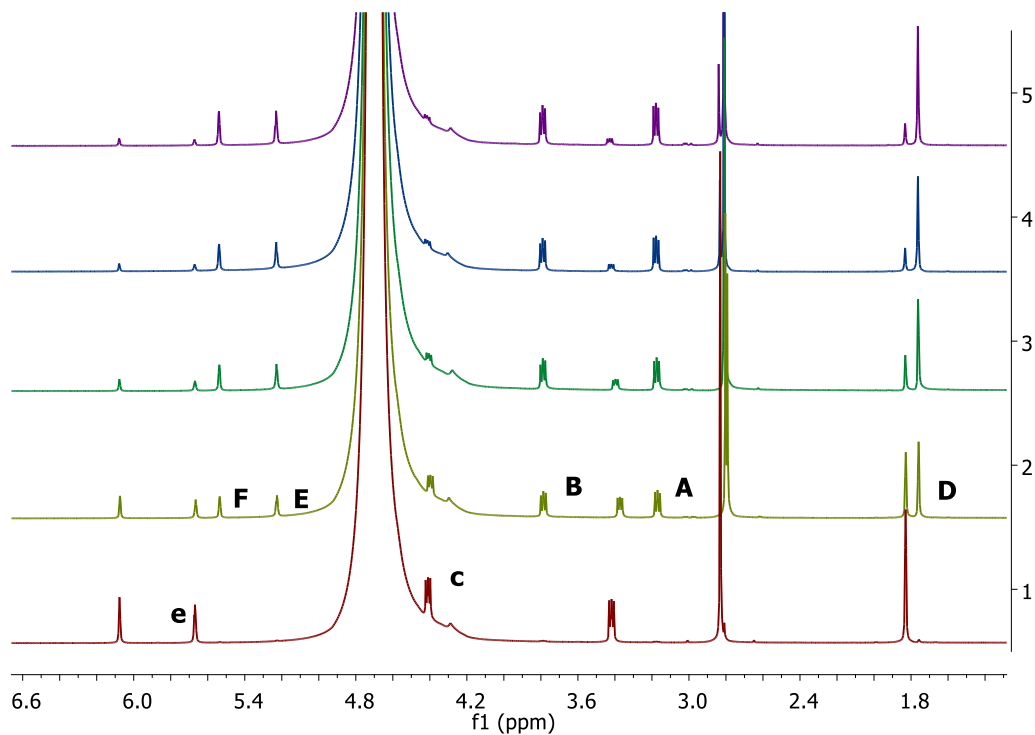


Figure 4.4 DMAEMA hydrolysis at 65°C in CO₂ saturated aqueous phase within 4h (pH=7.14)

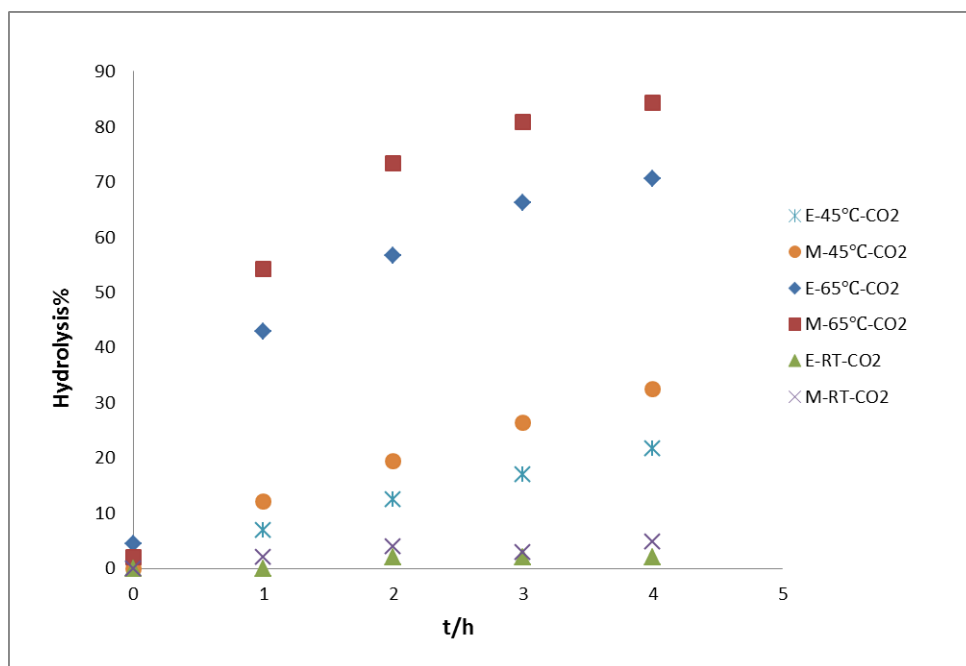
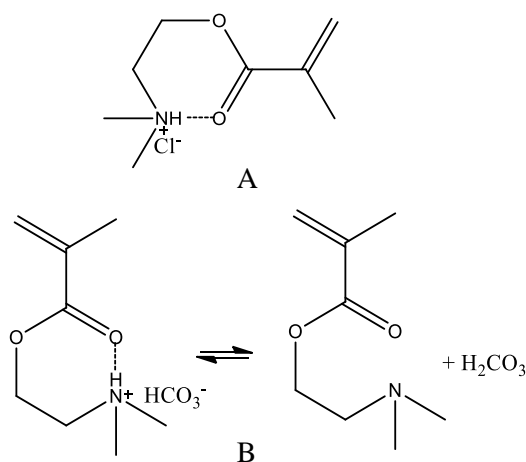
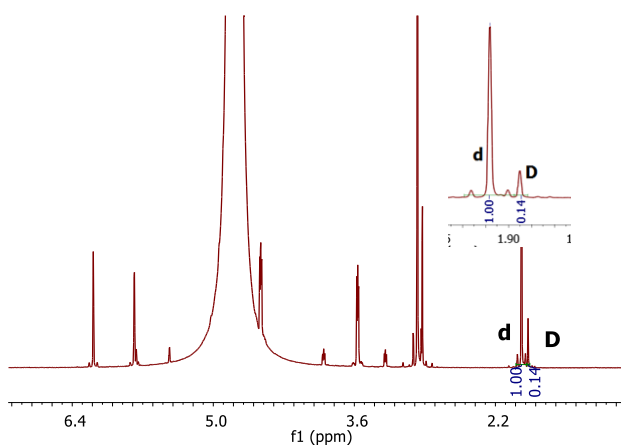


Figure 4.5 Temperature dependence of hydrolysis of DEAEMA/DMAEMA at CO₂ saturated acidity (M:DMAEMA; E:DEAEMA)

Table 4.4 Rate constants and half-life of hydrolysis of DMAEMA/DEAEMA

| | 65°C/CO ₂ | 45°C/CO ₂ | RT/CO ₂ |
|--------|--|--|--|
| DMAEMA | 1×10 ⁻⁴ s ⁻¹ /1.9h | 3×10 ⁻⁵ s ⁻¹ /6.4h | 3×10 ⁻⁶ s ⁻¹ /2.7d |
| DEAEMA | 8×10 ⁻⁵ s ⁻¹ /2.4h | 2×10 ⁻⁵ s ⁻¹ /9.6h | - |

**Scheme 4.4** Ring formation of DMAEMA upon HCl and CO₂ protonation**Figure 4.6** Hydrolysis of 84% HCl protonated DMAEMA (12%, pH=7.41)

One theory proposed by earlier researchers⁸ suggested that once the tertiary amine group was protonated, an intramolecular seven-member ring formation would be possibly promoted (Scheme 4.4 A) in chloroform solution, which made the ester group less susceptible to nucleophilic attack from a hydroxyl ion. In our system, CO₂ protonation was reversible. A similar ring formation (Scheme 4.4 B) was not of significance compared to hydrogen bonding with water in the protic environment. Evidence supporting this is shown in Figure 4.6, where 84% equivalent amount of HCl was used to imitate CO₂ protonation condition under 65°C and left for 4 hours at this temperature. NMR analysis showed 12% DMAEMA underwent hydrolysis compared to 84% in the case of CO₂, and the final chemical shift indicated that the remaining DMAEMA was almost 100% protonated. Once the 84% ester group was “trapped” into the ring confirmation

upon HCl protonation, it was no longer prone to hydrolysis but only the remaining 17% “free” DMAEMA molecular was susceptible to water attack and eventually most of them decomposed into methacrylic acid and dimethylaminoethanol within 4 hours. Under CO₂ protonation at 65°C, the 84% protonation efficiency was established in a dynamic equilibrium manner between the charged and neutral forms. Once the molecule was uncharged, the DMAEMA molecule immediately became unstable towards hydrolysis, and eventually the total hydrolyzed amount reached 84%. To define a relatively hydrolysis-safe operation window as shown in Figure 4.7, a broad pH range from 1~7 could keep the hydrolysis degree within ~10% with HCl protonation. If pH decreases to the low end (<1), the ester group might also be protonated and the ring formation would be no longer preserved, therefore triggering the acidic catalyzed mechanism. In a CO₂-saturated aqueous system, a temperature lower than 45°C could limit the hydrolysis to under 30~40%. However, lowering the temperature would significantly reduce the polymerization rate. A redox initiation system might offer a viable solution to this issue.

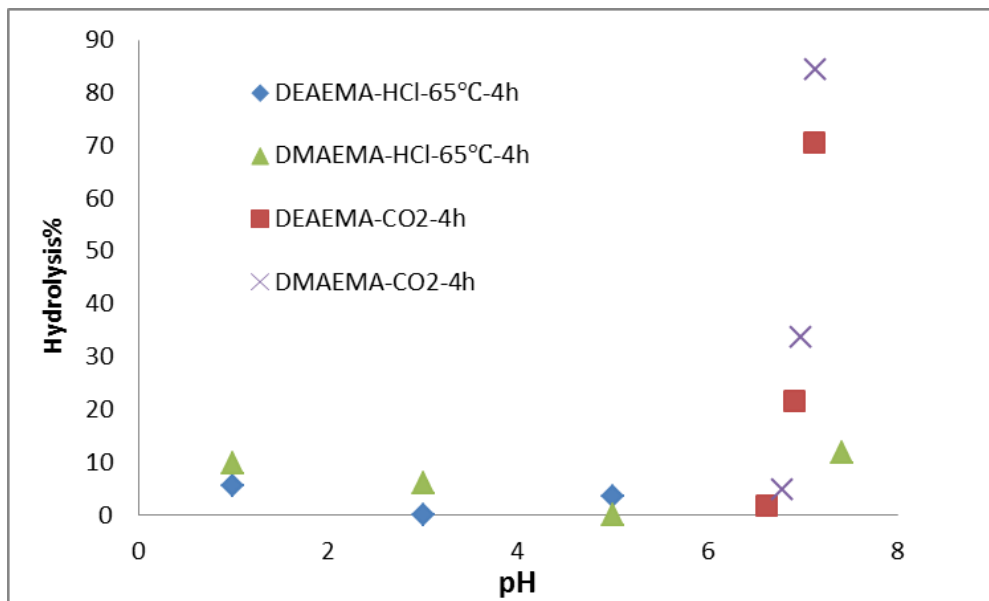


Figure 4.7 Hydrolysis degree under CO₂/HCl protonation at pH/temperature conditions

With an understanding of monomer hydrolysis and reversible protonation, the reason for inferior performance of DEAEMA/DMAEMA under CO₂ protonation can be more effectively addressed. Hydrolysis was believed to be the major cause due to loss of stabilizing tertiary amine groups and temporarily protonated DEAEMA/DMAEMA molecules, which were mainly responsible for the high degree of hydrolysis even when highly protonated at a relatively low pH. Considering the hydrolysis products, under the experimental pH conditions, poly(methacrylic acid) with a pK_{aH} of 5.5⁹ would not be fully protonated. The dimethylaminoethanol left in the aqueous phase could be protonated, as it was observed during the hydrolysis study, which showed that the peaks assigned to the dimethylaminoethanol showed a response in chemical shift to pH. The presence of the hydrolysis products could either increase the ionic strength of the continuous phase when moving freely in the aqueous phase which promotes latex aggregation, or if absorbed onto the particle surfaces could interfere with the electrostatic double layer. In both cases, latex stability would be compromised. In particular the presence of anionically charged poly(methacrylic acid) is of concern.

4.5 Conclusion

In a surfactant-free emulsion polymerization system, DEAEMA⁺HCO₃⁻ is a weaker stabilizer and a poorer nucleation agent compared to DEAEMA⁺Cl⁻, reflected by smaller particle size population. A high degree of monomer hydrolysis caused significant loss of the stabilizing tertiary amine groups and is believed to be the major cause of DEAEMA being less effective under CO₂ protonation in terms of producing stable and narrowly dispersed latexes.

With DMAEMA and DEAEMA being popularly employed in CO₂-responsive systems, it is necessary to quantify their degree of hydrolysis in the corresponding reaction conditions. ¹H NMR is a simple and effective method to study the hydrolysis by comparing the integration of the methyl group adjacent to the double bond of both monomers before and after hydrolysis. 84% of DMAEMA and 73% of DEAEMA were found to have hydrolyzed after 4 hours at 65°C in a CO₂-

saturated aqueous phase. The degree of hydrolysis was much lower at 45°C with a 33% loss of DMAEMA and 22% loss of DEAEMA at the same 4 hour time scale. Hydrolysis was almost negligible with CO₂ protonation at room temperature for both monomers.

DEAEMA protonation by CO₂ is a reversible process, which is responsible for the much higher degree of hydrolysis compared to that of HCl at 65°C, even with the same 84% overall protonation degree. With the irreversible protonation provided by HCl, a broad pH range of 1~7 at high temperature (65°C) can be considered as a suitable operational window with a hydrolysis degree controlled below 10% (4 hours), while choices with CO₂ protonation were limited to lower temperature (<45°C) with a reduced hydrolysis under 35% in case of DMAEMA and 25% for DEAEMA.

References

- (1) Zhu, S. *Macromol. Rapid Commun.* **2012**, *33*, 916–921.
- (2) Zhang, Q.; Yu, G.; Wang, W.-J.; Yuan, H.; Li, B.-G.; Zhu, S. *Macromolecules* **2013**, *46*, 1261–1267.
- (3) Pinaud, J.; Kowal, E.; Cunningham, M.; Jessop, P. *ACS Macro Lett.* **2012**, *1*, 1103–1107.
- (4) Fowler, C. I.; Jessop, P. G.; Cunningham, M. F. *Macromolecules* **2012**, *45*, 2955–2962.
- (5) Su, X.; Jessop, P. G.; Cunningham, M. F. *Macromolecules* **2012**, *45*, 666–670.
- (6) Pinaud, J.; Kowal, E.; Cunningham, M.; Jessop, P. *ACS Macro Lett.* **2012**, *1*, 1103–1107.
- (7) Van de Wetering, P.; Moret, E. E.; Schuurmans-Nieuwenbroek, N. M.; van Steenbergen, M. J.; Hennink, W. E. *Bioconjug. Chem.* **1999**, *10*, 589–597.
- (8) Van de Wetering, P.; Zuidam, N. J.; van Steenbergen, M. J.; van der Houwen, O. A. G. J.; Underberg, W. J. M.; Hennink, W. E. *Macromolecules* **1998**, *31*, 8063–8068.
- (9) Porasso, R. D.; Benegas, J. C.; van den Hoop, M. a. G. T. *J. Phys. Chem. B* **1999**, *103*, 2361–2365.

Chapter 5

Conclusions and recommendations for future work

5.1 Conclusions

A series of CO₂-switchable PMMA latexes was successfully prepared by surfactant-free emulsion polymerization using a small fraction of the functional comonomer DMAEMA. DMAEMA was protonated by strong acid (HCl) during the polymerization in order to prevent the high degree of hydrolysis that occurs under CO₂ protonation at the reaction temperature. The protonation also enhanced the partitioning of DMAEMA into the water phase and thus made it a more efficient surface active agent. The combined utilization of cationic initiator VA-044 and protonated DMAEMA enabled the stabilization of the colloidal system, with the resulting latex having high zeta potential above +50mV. The resulting latex showed very fast response to the triggers CO₂ and N₂, and both switching-on and switching-off cycles were completed within 5 min. The particle size, PDI, solids content as well as latex stability were fully recovered within the two switching cycles that were investigated (Figure 5.1). There were constraints in terms of the experimental conditions required in order to get particle size < 300nm, PDI < 0.1 and a successful recovery after two switching cycles. The ratio of VA-044:DMAEMA should be within the range of 1:8~1:2 and the overall N% (N_{DMAEMA}+N_{VA-044}) should be at least 1%. The solids content could be increased to 20% while still controlling the PDI below 0.1 at an increased temperature of 75 °C



Figure 5.1 Two switching cycles of CO₂-switchable PMMA latex (Entry N-5)

The particle size control was carried out by varying the DMAEMA:VA-061 ratio (18:1~0:1), overall N% (4%~1%), temperature (65 °C, 75 °C) and solids content (5%~20%). By fine tuning experimental conditions, the particle sizes were well controlled within the range 170~500 nm. One of the most significant achievements was that the resulting system did not require sonication for redispersion. Even agitation was not applied during the switching-on procedures. This is a major step toward industrial application of CO₂ switchable latex technologies.

5.2 Recommendations for future work

5.2.1 Continuing the use of azo initiators

It has been concluded in Chapter 3 that the monodispersity of the particles was mainly attributed to the fast initiation. The azo initiators (VA-044, VA-061 etc.) have demonstrated fast decomposition kinetics and a good incorporation into our emulsion system, with extensive benefits for providing additional stabilization and switchable properties. The PDI of the resulting latex experienced broadening (>0.1) when the temperature was reduced to 55°C during some experimental trials. The temperature recommended for the MMA system is around 65°C. At higher temperature such as 75°C, some foaming was observed even when there was no gas bubbling into the system.

5.2.2 Developing more techniques for surface group characterization

Our understanding of switchable latexes was significantly improved after the characterization work on functional monomers. However, characterization techniques suitable for studying surface composition of the polymer particles are still needed, specifically the tertiary amine groups. It remains a challenge to completely characterize latex particles, and techniques such as NMR and soap titration have their own limitations. The further development of new technology or new

combination of conventional technologies should be developed in order to fully understand the colloidal system.

5.2.3 Introducing new functional monomers as CO₂ responsive agent

NMR characterization on the degree of hydrolysis of the functional (switchable) groups was carried out on a new choice of monomer, N-[3-(dimethylamino)propyl]methacrylamide. Within 4 hours at 65 °C with CO₂ protonation, there was no hydrolysis observed (Figure 5.2). This stability towards hydrolysis has made it a promising candidate as a CO₂-switchable monomer. However, the corresponding homopolymer has complete solubility in water, which should be taken into consideration.

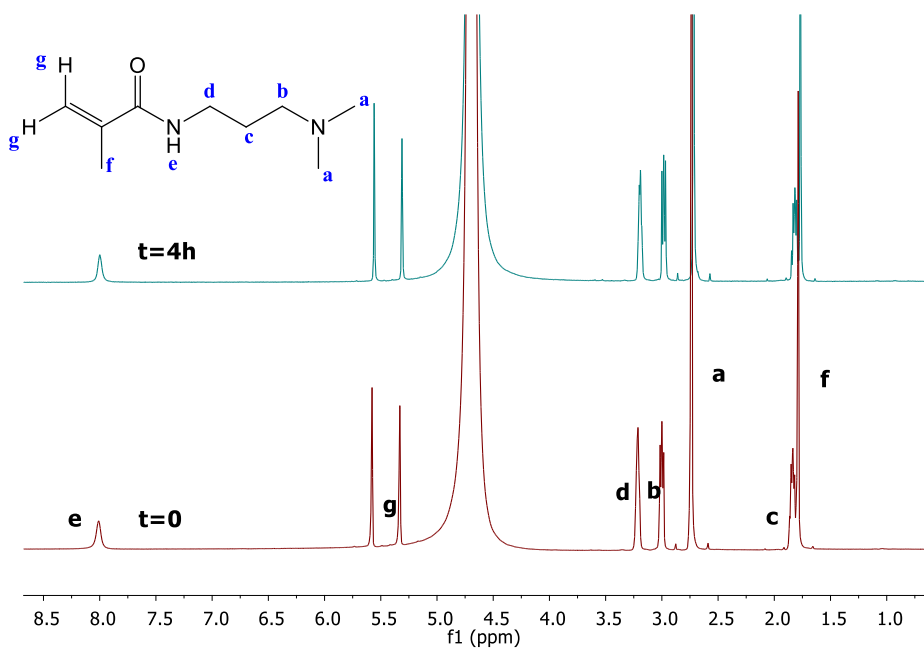


Figure 5.2 NMR determination of hydrolysis degree of N-[3-(dimethylamino)propyl]methacrylamide

5.2.4 Extension to more emulsion techniques

Towards the goal of industrial implementation, semi-batch approaches including using seeded emulsions should be further explored to achieve higher solids content. The system developed in this work has reached a solids content at 20% with excellent colloidal stability (zeta potential $\sim +50\text{mV}$). A seeded emulsion approach could extend the limit of achievable solids content in this surfactant-free emulsion polymerization, possibly to 40%.

5.2.5 Exploring low T_g materials

Low T_g materials such as the family of butyl methacrylate or butyl acrylate containing polymers are widely used in the coating and painting industry for film formation at room temperature. It remains a challenge to prepare low T_g CO_2 -switchable latex as the polymers on the particle surface tend to diffuse into each other during the switching-off process. A switching-on process will then become impossible once the particle surfaces fuse and particles lose their individual identity.

As discussed in Chapter 3, the amidine group inside the residual group of imitator VA-044 was probably not fully switched off during the N_2 purging. This provides an opportunity to find a window where the residual charge could possibly keep the particles apart efficiently even in the case of low T_g materials while the entire system could still present a switching-off response.

5.2.6 Potential application in drug delivery systems for cancer therapy

A tumour site produces higher levels of CO_2 than normal organs since the metabolism is accelerated by excessive growth of the tumour cells. There is a narrow pH range that a CO_2 switchable system could find its application as a responsive drug release system by careful choice of the pK_{aH} of the responsive agent. An ideal model would be that the acute response enables the drug to be released specifically to the tumour site. As soon as the system leaves the site, it could reversibly recover to a plasma-friendly medium.



5.2.7 High pressure CO₂ atmosphere for DMAEMA/DEAEMA systems

We have considered that increasing the CO₂ pressure to achieve a pH of 4 would lead to a “hydrolysis safe” condition and the protonation efficiency will also be greatly improved. According to the results in Chapter 3, however, as long as the DMAEMA/DEAEMA is not 100% protonated, the protonation equilibrium would slowly lead to a significant amount of hydrolysis. Therefore, high pressure might not be a suitable approach in terms of inhibiting monomer hydrolysis.

Appendix A

Zetasizer cell choice and proper sample dilution

Table A.1 Zeta-potential measurement using dip cell/ disposable zeta cell

| Cell Type/Sample | DTS1070-Dip Cell | DTS1060C-Clear Disposable Zeta Cell |
|----------------------------|---|--|
| |  |  |
| PMMA Latex/A-1-F | +56.5 mV | +78.9 mV |
| Zeta-Standard/-55(+/-5) mV | -53.6 mV | -62.5 mV |

It is advised that zeta-potential measured by dip cell is a more accurate read compared to the disposable zeta-cell, which tends to give higher absolute value.

Table A.2 Effect of sample concentration on particle size

| Sample dilution (Original sample 10wt%) | Weight concentration | Particle size(nm)/PDI |
|--|----------------------|-----------------------|
| 50ul to 1ml | 0.5% | 236.5/0.014 |
| 50ul to 4ml | 0.125% | 246.7/0.028 |
| 10ul to 2ml | 0.05% | 248.7/0.021 |

For particle size within the range 100 nm~1000 nm, proper sample concentration recommended by the official User Guide is 10^{-3} wt%~1 wt %, which is a broad range. Particle size experienced variation even though the concentration after dilution was inside this range. The sample

concentration adopted in this thesis work was chosen at 0.05% where the result of particle size stabilizes to successive dilution and the deviation from the higher concentration was negligible.

Appendix B

Rate constant and half-life calculation of DMAEMA/DEAEM monomer hydrolysis

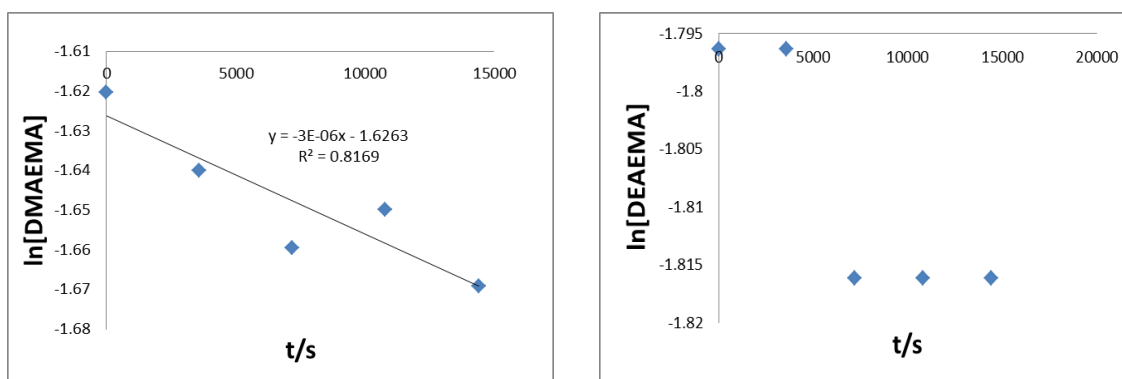
The monomer hydrolysis was regarded as a first-order reaction as water was far excess.

$$\ln[A] = -kt + \ln[A]_0$$

$$t_{1/2} = \ln 2/k$$

Where $[A]_0$ and $[A]$ are the concentrations of monomer DMAEMA/DEAEMA at time t_0 and t , k is the rate constant, $t_{1/2}$ is the half-life.

Plot $\ln[A]$ versus t , we can get the hydrolysis rate constant and half-life. (Concentrations used in all plots were in unit mol/L.)



*Data is too poor to be plotted.

Figure B.1 $\ln[\text{DMAEMA/DEAEMA}]$ vs. time at room temperature

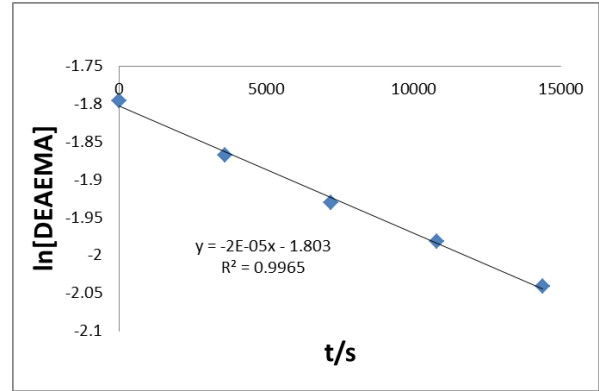
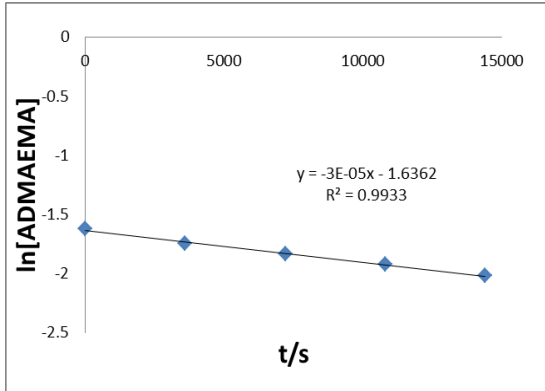


Figure B.2 $\ln[\text{DMAEMA}/\text{DEAEMA}]$ vs. time at 45°C

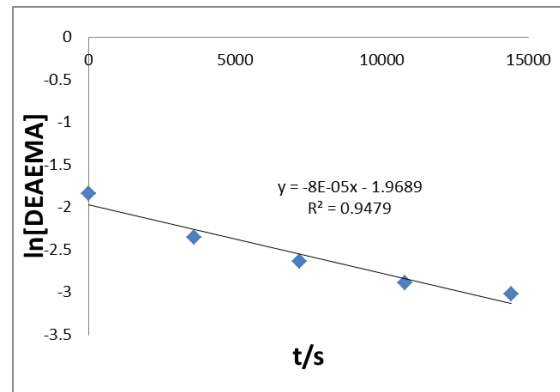
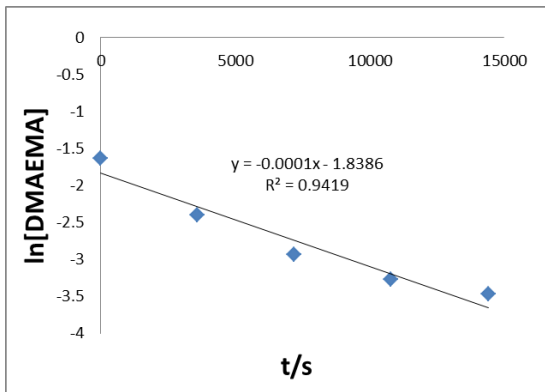


Figure B.3 $\ln[\text{DMAEMA}/\text{DEAEMA}]$ vs. time at 65°C

Appendix C

Replicate runs

In order to assure that the trends of particle size obtained were reliable, three experimental entries (random choices under different experimental formulations and conditions) were repeated to test the particle size deviations. Table C.1 illustrated the chosen entries and the particle size results of each replicate.

Table C.1 Particle size results of replicate runs

| Entry | Particle Size (nm) | Particle Size Mean (nm) | Deviation |
|-------|--------------------|-------------------------|-----------|
| N-2 | 247 | 248 | ±0.4% |
| N-2-R | 249 | | |
| N-7 | 267 | 277 | ±4% |
| N-7-R | 286 | | |
| S-3 | 262 | 265 | ±1% |
| S-3-R | 268 | | |

*Deviation=(Experimental result of each run – Particle size mean)/Particle size mean

The deviation was significantly small and the results of particle size in each replicate run were indeed repeatable.